

**Analysis of Crystallization of Paraffin Wax by Using Avrami Kinetic Model and
LFRA**

by

Mira Syamimi Binti Mazlan

Final report submitted in partial fulfillment of
the requirements for the
Bachelor of Engineering (Hons)
(Chemical Engineering)

MAY 2012

Universiti Teknologi PETRONAS

Bandar Seri Iskandar

31750 Tronoh

Perak Darul Ridzuan

CERTIFICATION OF APPROVAL

Analysis of Crystallization of Paraffin Wax by Using Avrami Kinetic Model and LFRA

By

Mira Syamimi Binti Mazlan

A project dissertation submitted to the

Chemical Engineering Programme

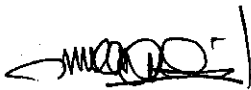
Universiti Teknologi PETRONAS

In partial fulfillment of the requirement for the

BACHELOR OF ENGINEERING (Hons)

(CHEMICAL ENGINEERING)

Approved by,



(Dr. Lukman Ismail)

UNIVERSITI TEKNOLOGI
PETRONAS

TRONOH, PERAK

May 2012

CERTIFICATION OF ORIGINALITY

This is to certify that I am responsible for the work submitted in this project, that the original work is my own except as specified in the references and acknowledgments, and that the original work contained herein have not been undertaken or done by unspecified sources or persons



MIRA SYAMIMI BINTI MAZLAN

ACKNOWLEDGEMENT

First and foremost, praises be to Allah S. W. T whom had poured His tremendous blessing and wisdom upon the author throughout her whole life as a student. Through Him everything is possible and this project can be completed despite of those obstacles and hardship.

The author would like to express her greatest gratitude to her project supervisor, Dr. Lukman Bin Ismail for his guidance and supervision. The project gives author new valuable experiences during the period in finishing the project. Thank you for the time that you had spent to guide and supervise the author throughout the whole semester.

Apart the project supervisor, the author would also like to express her appreciation to the lab technologist and technicians for their willingness to share their knowledge and provide help to the author in handling the equipments used. The authors also wish to acknowledge the materials, equipment and financial support provided by Department of Chemical Engineering, UTP and Universiti Teknologi PETRONAS. A grateful appreciate is addressed to all who had contributed to the accomplishment of this project, for the constant encouragement and timely help throughout the whole semester for FYP I and FYP II.

Last but not the least, the author would like to thank her parents, Mr. Mazlan Majid and Mrs. Rohana Mat Isa whom had supported and motivated her in many kind of ways and the main reason for the author to keep on pushing herself towards success. The author could not have done it without them. Thank you for the endless love.

ABSTRACT

For many years, deposition of paraffin wax in oil and gas pipelines has been the major problems in petroleum industries that mostly related to pump, wax blockage in pipelines and equipments failure. The objectives of this work are to study the effect of certain parameters such as temperature differential, different wax compositions and different type of solvents towards wax crystallization and also to understand the effects against wax properties itself such as hardness, break load, adhesiveness and viscosity that LFRA Texture Analyzer and viscometer could produce. The kinetics and mechanism of wax crystallization is further studied in accordance to Avrami Theory. For the experiment of investigating the effect of temperature differential, there will be two fixed parameters which are fixed T_{\min} and Fixed T_{\max} . The wax compositions used is fixed which is 17%. Firstly the T_{\min} is fixed to 2°C while the T_{\max} varied from 60, 70 to 80°C. Secondly, the T_{\max} is fixed to 70°C and the T_{\min} varied from 5, 10 to 15°C. For the experiment the effect of wax compositions, the wax compositions is varied from 5, 10, 15 to 20% and diesel is used as the model-oil. Lastly, for the experiment the effect of different types of solvents, four different solvents are used which are diesel, heptanes, hexane and octane. The wax compositions used is fixed which is 17%. The results indicate that for temperature differential have two opposite effects on the results of wax deposition: For fixed T_{\min} , wax deposition and the viscosity decreasing as the temperature difference increasing; for fixed T_{\max} , wax deposition and the viscosity are increasing as the temperature difference increasing. For the second experiment, the wax deposition and the viscosity are increasing with the increase of the wax composition and this is well expected. As for the experiment of different types of solvents, the wax deposition is highest in the diesel but for the other solvent, as the carbon chain number is increasing from hexane, heptanes to octane, the wax deposition and the viscosity is decreasing. The growth rate, K is increasing while the Avrami exponent, n is decreasing as the wax deposition is increasing. For the LFRA texture analysis, the hardness and the break load is increasing with the increase of the wax deposition while the adhesive force is decreasing as the wax deposition is increasing.

TABLE OF CONTENT

ACKNOWLEDGEMENT	iv
ABSTRACT	v
CHAPTER 1: INTRODUCTION	
1.1 Background of Study	1
1.2 Problem Statement	2
1.3 Aim and Objectives	2
1.4 Scope of Study	3
CHAPTER 2: LITERATURE REVIEW	
2.1 Theory and Mechanism of Wax Crystallization	4
2.2 Avrami Theory	5
CHAPTER 3: METHODOLOGY	11
3.1 Experimental Method	12
3.1.1 Effect of temperature differential towards the wax crystallization	12
3.1.2 Effect of wax composition towards the wax Crystallization	12
3.1.3 Effect of different types of solvents towards the wax crystallization	13
3.2 Equipments Used	14
3.2.1 Leatherhead Food Research Association (LFRA)	14
3.2.2 Viscometer	17
3.2.3 Chiller	18

3.2.4 Hot water bath	18
3.3 Key milestone	19
3.3.1 Timelines for FYP I	19
3.3.2 Timelines for FYP II	20
CHAPTER 4: RESULTS AND DISCUSSIONS	21
4.1 Effect of temperature differential	21
4.1.1 Fixed Tmax	21
4.1.2 Fixed Tmin	24
4.2 Effect of wax compositions towards wax crystallization	26
4.3 Effect of different types of solvents	28
4.4 LFRA Texture Analysis	31
CHAPTER 5: CONCLUSION AND RECOMMENDATION	35
REFERENCES	38
APPENDIXES	40

LIST OF FIGURES

Figure 1	Wax deposition occurs when the inner wall temperature is below the cloud point temperature (Hyun, 2008)	2
Figure 2	Thickness of deposition changing with time at different wall temperature (Oil temperature 45°C) (Guozhong et al., 2008)	7
Figure 3	Effect of oscillation frequencies on wax deposition for a range of paraffin content (Ismail et al., 2008)	8
Figure 4	The Avrami plots for different wax content showing the effect of oscillation frequencies (Ismail et al., 2008)	9
Figure 5	Paraffin Wax	11
Figure 6	A generalized texture profile analysis curve from the Instron Universal Testing Machine. A1, area 1; A2, area 2; A3, area 3. The dotted lines indicate the times at which hardness is measured (Pons and Fiszman, 1996)	16
Figure 7	Leatherhead Food Research Association Texture Analyser (LFRA)	16
Figure 8	Viscometer	17
Figure 9	Chiller	18
Figure 10	Hot water bath	18
Figure 11	Graph of wax deposits (wt%) vs time for the experiment the effect of temperature differential towards wax crystallization (T_{max} is fixed: 70°C. T_{min} varied: 5, 10, 15°C)	22
Figure 12	Avrami plot for the experiment the effect of temperature differential towards wax crystallization (T_{max} is fixed: 70°C. T_{min} varied: 5, 10, 15°C)	22
Figure 13	Graph of temperature difference vs viscosity for the experiment effect of temperature differential (Fixed T_{max}). ΔT : 55, 60, 65°C	23
Figure 14	Graph of wax deposits (wt%) vs time for the experiment the effect of temperature differential towards wax crystallization (T_{min} is fixed: 2°C. T_{max} varied: 60, 70, 80°C)	24

Figure 15	Avrami plot for the experiment the effect of temperature differential towards wax crystallization (T_{\min} is fixed: 2°C. T_{\min} varied: 60, 70, 80°C)	24
Figure 16	Wax deposition inside the beaker	25
Figure 17	Graph of wax deposits (wt%) vs time (min) for the experiment the effect of different wax composition towards wax crystallization (wax compositions: 5, 10, 15 and 20%)	26
Figure 18	Avrami Plot for the experiment the effect of different wax composition towards wax crystallization (wax compositions: 5, 10, 15 and 20%)	26
Figure 19	Graphs of viscosity vs wax composition (wax compositions: 5, 10, 15 and 20%. Model oil: Diesel)	27
Figure 20	Graph of wax deposits (wt%) vs time (min) for the experiment the effect of different types of solvents towards wax crystallization (Solvents: Diesel, Octane, Heptane and Hexane. Wax composition: 17%)	28
Figure 21	Avrami Plot for the experiment the effect of different types of solvents towards wax crystallization (Solvents: Diesel, Octane, Heptane and Hexane. Wax composition: 17%)	29
Figure 22	Graphs of solvent vs viscosity for the experiment the effect of different types of solvents towards the wax crystallization. (Solvents: Diesel, Octane, Heptane and Hexane. Wax composition: 17%)	29
Figure 23	Graph of texture analysis from LFRA Texture Analyzer for the experiment effect of different wax composition. Wax compositions: 20%. Model-oil used: Diesel.	31
Figure 24	Graphs of texture analysis for the experiment effect of different wax compositions. (Wax composition: 5, 10, 15 and 20%. Model-oil used: Diesel)	32
Figure 25	Graph of texture analysis from LFRA Texture Analyzer for the experiment effect of different type of solvents. Solvent used: Diesel. Wax composition: 17%	33
Figure 26	Graph of texture analysis for the experiment effect of different type of solvents. (Solvents used: Diesel, Octane, Heptane and Hexane). Wax composition: 17%	34

LIST OF TABLES

Table 1	The average wax deposition under different temperature differential between the oil and the wall when the oil temperatures are 50°C, 45°C and respectively (Guozhong et al., 2008).	8
Table 2	Avrami parameters for crystallization	10
Table 3	Compositions and properties of paraffin wax	11
Table 4	LFRA Standard setting	15
Table 5	Parameters and Units of Instrumental Texture	16
Table 6	Temperature difference is 5°C and 70°C. Mo=104.16g	21
Table 7	Extracted Avrami parameters for the effect of temperature differential (Fixed T_{max})	23
Table 9	Extracted Avrami parameters for the effect of temperature differential (Fixed T_{min})	25
Table 9	Extracted Avrami parameters for the effect of wax composition	27
Table 10	Extracted Avrami parameters	30
Table 11	Texture analysis for effect of different wax compositions	31
Table 12	Texture analysis for different type of solvents	33

CHAPTER 1

INTRODUCTION

1.1 Background study

Many researches have been done regarding paraffin wax deposition in the pipeline of the petroleum productions. As for the properties of the paraffin wax, it is normal alkanes with straight chain molecules and single C-C bond. It is in solid form when the carbon number is from C₁₈ and above which is then known as waxes. Paraffin waxes have orthorhombic, hexagonal, monoclinic and triclinic structures (Richter *et al.*, 1996). Crystallization of paraffin wax is actually an example of solid-liquid phase equilibrium. It is explained in term of established principle of thermodynamic of solutions where the solution of higher molecular weight hydrocarbon in lower molecular weight hydrocarbon that acts as a solvent. Generally, high molecular weight hydrocarbon precipitate whenever the carrying capacity of the fluid solvent decreases (Won *et al.*, 1985).

The wax deposition of the crude oil in the pipelines makes the flow area smaller and smaller by time that will then influences the transportation capacity and the operation safety of the pipelines (Burger *et al.*, 1981). The presence of wax crystals changes the flow behaviour of the crude oil from Newtonian to non-Newtonian. The wax crystals usually lead to higher viscosity with increased energy consumption for pumping and decreased capacity of the production. In addition, if the oil is cooled during transportation, the wax crystals tend to deposit on the colder pipe wall. Wax deposits can lead to increased pipeline roughness, reduced effective diameter, more frequent pigging requirement and potential blockage. If these deposits get too thick, they can reduce the capacity of the pipeline and cause lots of problems (Won *et al.*, 1985).

1.2 Problem Statement

Crystallization of paraffin wax has been the same problem encountered which influenced the transportation capacity, the operation safety of the crude oil pipelines and huge economic losses to the petroleum industry through the cost of chemicals, reduced production choking of the flowlines, equipment failure and extra manpower attention. The incipient gel grows as time progresses while there are radial thermal and mass transfer gradients as a result of heat losses to the surroundings as shown in **Figure 1**. By studying the effect of certain parameters towards the wax crystallization could help on further understanding the mechanisms and kinetic analysis of the wax crystallization. Thus the problem regarding wax crystallization could be controlled and reduced. Beside

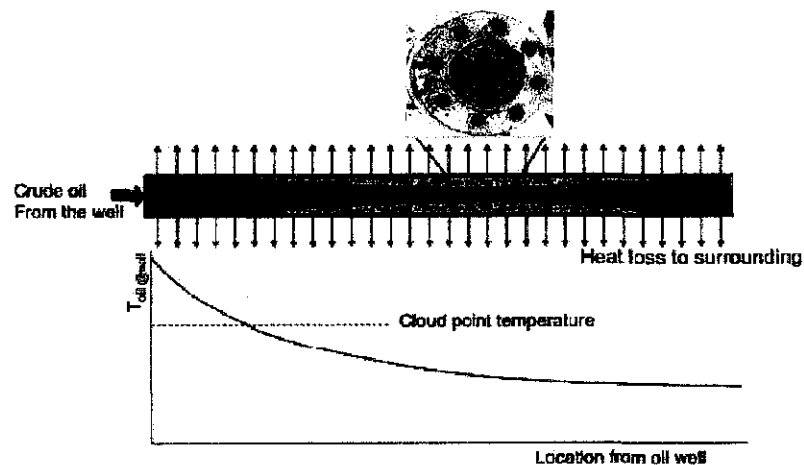


Figure 1: Wax deposition occurs when the inner wall temperature is below the cloud point temperature (Hyun, 2008)

1.3 Aim and Objective

The aim of this work is to study the effect of certain parameters towards the crystallization of paraffin wax and understand the effects against wax properties itself such as hardness, adhesiveness and viscosity that LFRA Texture Analyzer and viscometer could produce. Not to forget to further understand the kinetics and mechanism of wax crystallization in accordance to Avrami Theory. The specific objectives of the project are:

- i. To study the effect of temperature difference towards the paraffin wax crystallization
- ii. To study the effect of wax composition towards the wax crystallization
- iii. To study the effect of different types of solvents towards the wax crystallization
- iv. To examine the texture of the crystallization of paraffin wax by using Leatherhead Food Research Association Texture Analyzer (LFRA)
- v. To examine the viscosity of the solution by using viscometer

1.4 Scope of Study

Basically, the scope of study is to determine characteristic of the wax crystallization and also to study the cause and effect of certain parameters towards the crystallization of paraffin wax. Experiment will be conducted to study the effect of temperature differential, different wax composition and different types of solvents towards the wax crystallization. For the experiment the effect of temperature differential towards the wax crystallization, there are two fixed variable conducted. Firstly, the T_{max} is fixed to 70°C. So the range for T_{min} varied from 5, 10 to 15°C. Secondly, the T_{min} is fixed to 2°C. So the range of T_{max} is varied from 60, 70 to 80°C. The oil enters the pipeline at 60-70°C and the ocean water is much colder (4°C in deep water) especially in colder region. So from here we could examine the wax precipitation due to different temperature differential, ΔT . For the experiment of the effect of wax composition towards wax crystallization, the ranges of wax composition are from 5, 10, 15 and 20%. In the real world, the wax content of crude oil is generally less than 20% (Leontaritis *et al.*, 1988). For the experiment of the effect of different solvents towards wax crystallization, four different solvents are used which are hexane, heptane, octane and diesel. Apart from that, machines such as LFRA and viscometer will be used to examine the texture of the wax crystallization and the viscosity of the solution due to the effect of the experiments that will be conducted as mentioned above.

CHAPTER 2

LITERATURE REVIEW

2.1 Theory and Mechanism of Wax Crystallization

The paraffin deposition and wax plugging on the inner walls of the subsea crude oil pipelines present a costly problem in the production and transportation of oil and has been widely reported and studied by researches in past decades. For subsea pipelines, in particular it has become especially important to solve the issue of wax build-up as large scale oil production in colder regions will be faced more severe wax precipitation (Smith and Ramsden, 1978; Asperger *et al.*, 1981). It required lots of time for the removal of the deposited wax and to address the reduction in flow rate that it causes as well as to avoid the eventual loss of a pipeline where it becomes completely clogged (Aiyejina *et al.*, 2011). In order to further understand the problems, significant researches been done on the mechanism governing wax deposition in pipelines and more methods of inhibiting the formation of wax in pipeline walls have been studied to find the most efficient and cost-effective means of maintaining pipelines prone to wax deposition. It is important to study the causes and effect of certain conditions towards the crystallization of paraffin wax so that it could be reduced and controlled.

The main factor that controls the saturation of paraffin wax is mainly the temperature. When the temperature of the crude oil drops below the paraffin solubility limit, known as the cloud point, the heaviest-paraffin fractions precipitate out of the solution as solid wax crystals (Kristofer *et al.*, 2005). In a simpler word, paraffin wax crystallization occurs when the temperature of the oil drops below the Wax Appearance Temperature (WAT). Gelation occurs when paraffin crystals interact to form networks which entrain the remaining liquid oil and impart solid like mechanical properties to the fluid (Kristofer *et al.*, 2005). In petroleum transport pipelines, paraffin gel deposits form at the cold interior surface of the pipe wall and increase in thickness and hardness by time until a complete blockage is formed. As mentioned before, wax precipitation

within pipelines at and below the Cloud Point or WAT can lead to gelling that inhibits flow by causing significant non-Newtonian behaviour and increasing effective viscosities as the temperature of a waxy crude oil approaches its Pour Point which is the temperature when fuel gels (Pederson and Ronningsen, 2003).

Azevedo and Teixeira (2003) did a critical review of wax deposition mechanism starting with wax deposition by molecular diffusions as described by Burger *et al.* (1981). In this review, it is acknowledge that in most model of wax deposition, molecular diffusion is a main mechanism. It is assumed that for the flow of crude oil in the turbulent regime, the turbulent diffusivities of momentum, chemical species and temperature will lead to a uniform distribution of velocity, temperature and concentration profiles in a pipe cross-section. Therefore, the transport of wax will be controlled by the gradients prevailing at the laminar sub-layer close to the wall (Azevedo and Teixeira, 2003). Since wax solubility decreases with the temperature, there will also be concentration gradient established by the temperature gradient within the pipelines, with the cooler region near the wall having the lowest concentration of wax in the liquid phase. This is what leads to the molecular diffusion of wax from the bulk fluid to the walls of the pipelines (Aiyejina *et al.*, 2011).

2.2 Avrami Theory

The objective of this project is to study the effect of parameters such as temperature, wax composition and different types of solvents towards the crystallization of paraffin wax and relate the experiments by fully understand the mechanism and kinetics of the wax crystallization in accordance to Avrami Theory. The Avrami phase transition equation is a well known principle in describing the crystallization kinetics. The volume fractions of crystalline material, X also known widely as the degree of crystallinity can be written as

$$1 - X = e^{-E} \quad (1)$$

where E is the average number of fronts of all such points in the system. For low degree of crystallinity, a useful approximation is $X \approx E$.

For the bulk crystallization of polymers, E in the exponent may be considered the volume fraction of crystalline materials, V_t

$$1 - X = e^{-V_t} \quad (2)$$

For either instantaneous or sporadic nucleation, Eq. (2) can be written as

$$1 - X = e^{-Kt^n} \quad (3)$$

Where K is the growth rate and n is the Avrami exponent, which depends not only on the structure of the crystals but also on the nature of the nucleation (Avrami, 1940). The Avrami exponent, n , is the phenomenological index of crystallization which can be used to distinguish between different mechanisms of crystallization (Campus *et al.*, 2003). For example, when $n=1$ it corresponds to rod like growth from instantaneous nuclei whereas $n=3$ or 4 refers to spherulitic growth from either sporadic or instantaneous nucleation (Sharples, 1966). For polymer and organic systems an n -value of 2 or 3 indicates two or three dimensional nucleation of the crystals nucleus. However, the size and appearance changed abruptly from spherulitic to rod-like as the temperature of crystallization was increased.

In this study, the degree of crystallinity is measured by the relative wax composition, δ_r , defined as the mass fractions of the depositions on the wall divided by the initial mass of the wax-oil liquid

$$\delta_r = \frac{\delta_t - \delta_0}{\delta_\infty - \delta_0} \quad (4)$$

where δ_t is the total deposition at time t (min), δ_∞ the maximum or asymptotic deposition obtained from the deposition curves when the asymptotic condition state has been achieved. δ_0 is the initial mass of the wax content in liquid.

Replacing X by δ_r and taking log for both sides in Eq. (3) it becomes,

$$\log[-\ln(1 - \delta_r)] = \log K + n \log(t) \quad (5)$$

By plotting the left side in Eq. (5) versus $\log(t)$, the slope of the straight line, n , and the intersection, K , can be obtained. This information can be used to evaluate the wax deposition process. Wax deposition experiment can be used to determine the thickness of the wax deposition layer. For example, the one of the parameters that we are going to study the effect of it towards crystallization of paraffin wax is temperature differential, ΔT . This has been done by previous researchers. By taking the oil temperature is 45°C and the differences in temperature between the oil and the wall are 3°C , 5°C and 8°C in (a), (b) and (c) respectively, the change curves of the wax deposition layer thickness with time are shown in Figure 2

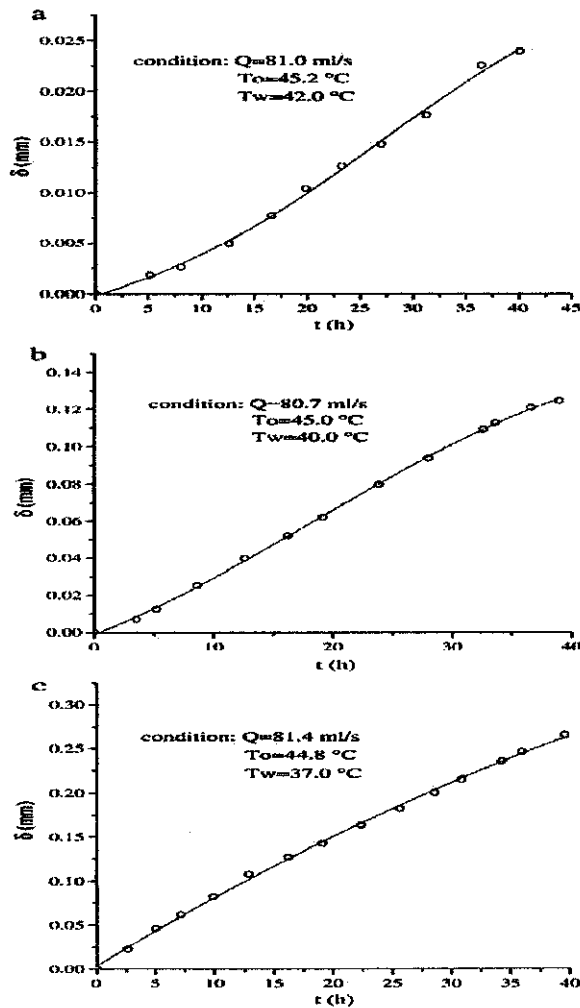


Figure 2 : Thickness of deposition changing with time at different wall temperature (Oil temperature 45°C) (Guozhong *et al.*, 2008)

It can be seen from the graph that the wax deposition layer thickness increases proportionally with time. The higher the temperature differential, the larger the wax deposition rate.

Table 1 : The average wax deposition under different temperature differential between the oil and the wall when the oil temperatures are 50°C, 45°C and respectively (Guozhong *et al.*, 2008).

Oil Temperature (°C)	Average wax deposition layer thickness (mm)		
	Difference in temperature between the oil and wall (°C)		
	3	5	8
50	0.0000	0.0418	0.1673
45	0.0143	0.0766	0.1607
40	0.0822	0.1333	0.0000
35	0.0000	/	/

The other parameter is the effect of wax composition towards the wax crystallization. The result is also based on previous research done by (Ismail *et al.*, 2008). But the main focus of the research is to asses the effect of baffle oscillation on the wax deposition.

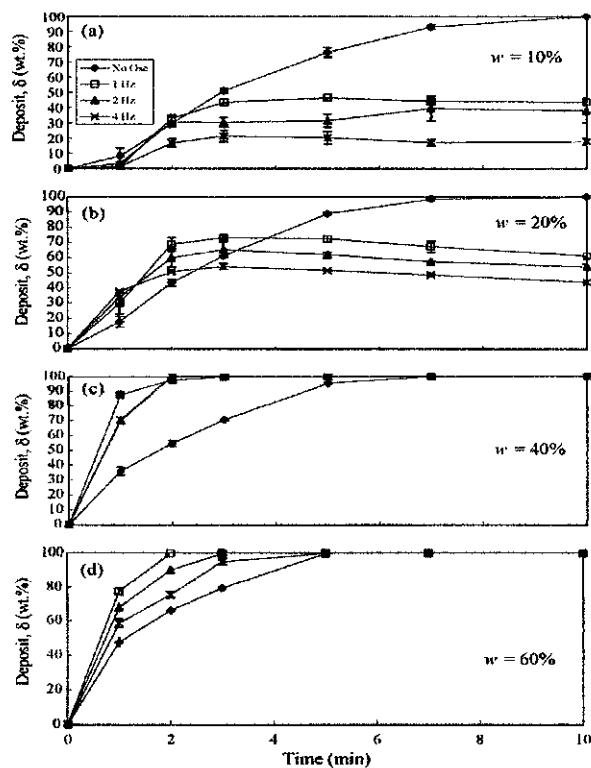


Figure 3: Effect of oscillation frequencies on wax deposition for a range of paraffin content (Ismail *et al.*, 2008)

Since the results from the graph indicates the effect of oscillation towards the wax crystallization, just take a look on the graph without oscillation. From the graph we could see that the higher paraffin content, the more wax deposits produced at any given time and faster the deposition rates. The increased on paraffin wax content means more wax molecules to produce more wax crystals. While below is the graph by plotting $\log[-\ln(1 - \delta_\tau)]$ versus $\log(t)$ using the Avrami Theory.

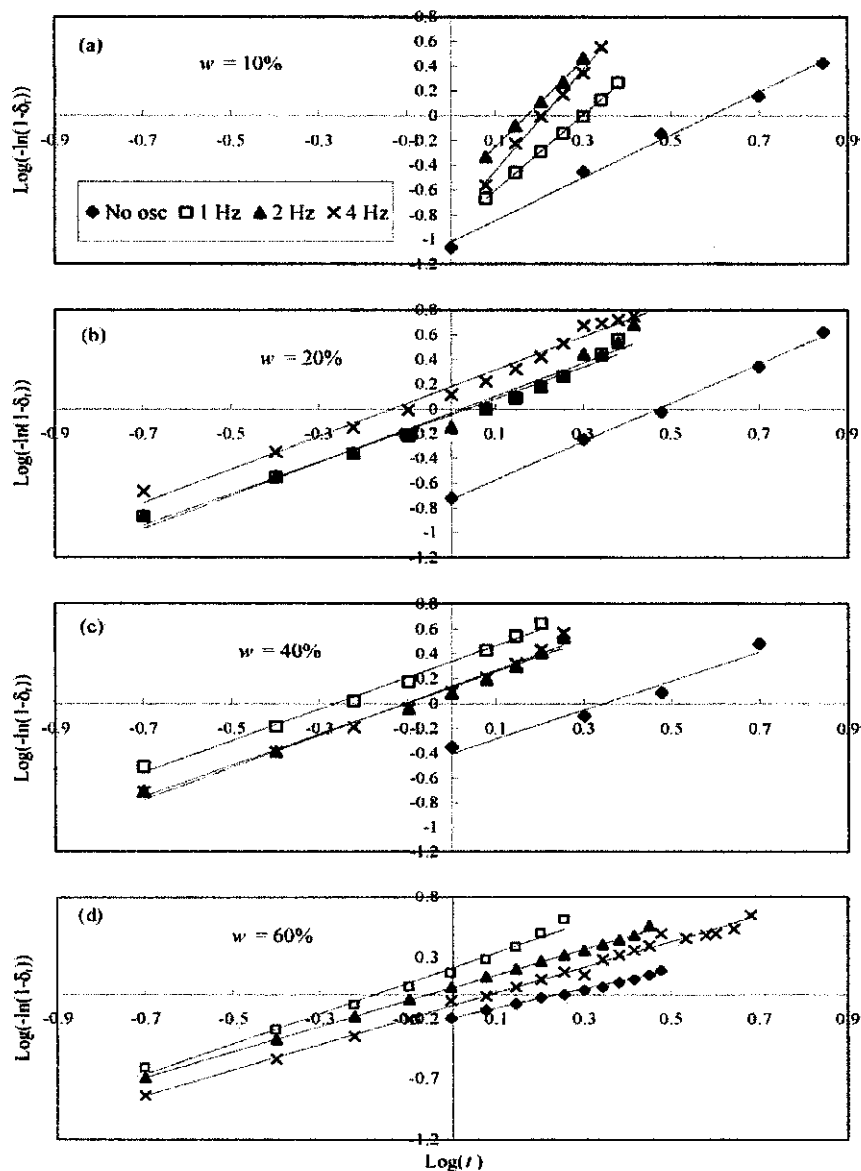


Figure 4 : The Avrami plots for different wax content showing the effect of oscillation frequencies (Ismail *et al.*, 2008)

This Avrami plots showing the effect of oscillation frequencies, so just take a look on plot of without oscillation. By analysing the growth phase curves by using the Avrami theory some crystallization kinetics can be extracted. The Avrami exponent (n) and the rate constant (K) are extracted from the plots as mentioned before where the slope of the straight line, n , and the intersection, K . Generally, the growth rate, K increases with the wax content in the solution. This is expected as the higher wax concentration will lead to more wax crystals thus higher crystallization rate. The Avrami exponent decreases with the increase of the wax concentration in the solution (Ismail *et al.*, 2008). The value of Avrami exponent, n is to decent whether the crustallization process is heterogeneous or homogeneous and also the type of crystallite morphology formed (e.g. rod, disc, sphere and sheaf). The following table gives a list of Avrami exponent and their morphologies.

Table 2: Avrami parameters for crystallization (Hay, 1971)

Crystallization mechanism	n	Growth form
Spheres		
Sporadic	4	Three dimensions
Instantaneous	3	Three dimensions
Discs^a		
Sporadic	3	Two dimensions
Instantaneous	2	Two dimensions
Rods^b		
Sporadic	2	One dimension
Instantaneous	1	One dimension

^a Constant thickness

^b Constant radius

The other studies which include the effect of different types of solvent towards the wax crystallization, the texture analysis of the wax crystallization and the viscosities of the solutions have been examined in this work where the experiments have been conducted in order to get the exact data.

CHAPTER 3

RESEARCH METHODOLOGY

3.1 Experimental Method

Firstly before starting the experiment, the properties of the paraffin wax need to be determined. To determine the melting range of the paraffin wax, the sample of solvent-wax will be filled in a beaker to be heated preferably at lower heat. The first sign of liquid within the beaker is indicating the melting point of the wax. The melting point will be recorded until all the wax is melted and when the final solid melted, that is the final range of melting temperature. To get more accurate data, the wax appearance temperature is determined by using Differential Scanning Calorimetry. DSC measures the heat flow from or to the sample when the sample is heated or cooled. Since crystallization will give out heat, it will show up in the DSC curve as an exothermic peak during cooling. Once the DSC has completed the test, a graph will be produced. As the oil sample is cooled from the maximum temperature, the heat trace measures the energy at each temperature. Once the paraffins align themselves and begin to form crystals, energy in the form of heat is given off. The exothermic reaction of crystallization is recorded. This temperature is determined to be the wax appearance temperature (WAT). By using DSC, the result is more accurate less time-consuming rather than by using the manual method by examined visually through a microscope for crystal formation where the WAT is determined as the temperature at which the crystals first appear.

Table 3: Compositions and properties of paraffin wax

Typical Carbon number	18-36
Average molecular weight	350-430
Melting point ranges (°C)	50-65



Figure 5: Paraffin Wax

3.1.1 Effect of temperature differential towards the wax crystallization

For the experiment the effect of temperature differential towards the wax crystallization, there are two fixed variables conducted. The wax composition used is fixed which is 17% and the solvent used is diesel. Firstly, the T_{\max} is fixed to 70°C. So the range for T_{\min} varied from 5, 10, to 15°C. Secondly, the T_{\min} is fixed to 2°C. So the range of T_{\max} is varied from 60, 70 to 80°C. The ranges temperature of T_{\min} and T_{\max} is controlled by using both chiller and temperature-controlled water bath as well as thermometer to monitor the temperature of wax-oil solution. T_{\min} refers to the wall temperature (which is controlled by the chiller) while T_{\max} refers to the temperature of the wax-oil solution (which is controlled by the temperature-controlled water bath). The typical experiment duration is 10 minutes and three wax deposits measurements are conducted at an interval of 1 minute for the initial 3 minutes followed by two measurements taken at an interval of 2 minutes for the middle 4 minutes and finally one measurement taken at the end of experiment time of 10 minutes. When carrying out measurements of wax deposition, the experiment is stopped and the non-crystallized wax-oil was drained out of beaker and weighed. The crystallized wax inside the column is determined by the difference between the weight of the empty beaker and the weight of the beaker with the deposit. After the measurement, the experiment is restarted by recombining the solid deposits with the liquid part

3.1.2 Effect of wax composition towards the wax crystallization

Firstly, for this experiment, the solvent is fixed where the solvent used is diesel. The wax sample was grinded into smaller particles to ease liquefaction process. A 150 ml beaker is weighed and the electronic scale was set to 0 before the diesel will be poured into. The grinded waxes were carefully sprinkled into the beaker until it is measured precisely at 2.5 grams (5% wax composition).

The diesel was slowly and carefully poured into the particular beaker until measured precisely the electronic scale showing 50 grams. The beaker opening was quickly wrapped with aluminum foil. The beaker is then heated up to in range of 50°C on the laboratory hot plate until all the wax melted. The solution is waited until homogeneous then cooled off to room temperature. The typical experiment duration is 10 minutes and three wax deposit measurements will be conducted at an interval of one minute for the initial three minutes followed by two measurements taken at an interval of two minutes for the middle four minutes and finally one measurement taken at the end of the experiment time of 10 minutes. When carrying out measurements of wax deposition, the experiment was stopped and the non-crystallized wax-oil was drained out of beaker and weighed. The crystallized wax inside the beaker was determined by the difference between the weight of the empty beaker and the weight of the beaker with the deposit. After the measurement, the experiment was restarted by recombining the solid deposits with the liquid part and the mixture was reheated to 50°C. The procedure was continued for different wax composition; 10, 15 and 20%.

3.1.3 Effect of different types of solvents towards the wax crystallization

Firstly, for this experiment, the wax composition is fixed to 17%. The first procedure was the same as mentioned above where the wax sample was grinded into smaller particle to ease liquefaction process. A 150 ml beaker was weighed and the electronic scale was set to 0 before the diesel will be poured into. The grinded waxes were carefully sprinkled into the beaker until it was measured precisely at 8.5 grams (17% wax composition). The diesel was slowly and carefully poured into the particular beaker until measured precisely the electronic scale showing 50 grams. The beaker opening was quickly wrapped with aluminium foil. The beaker was then heated up to in range of 50°C on the laboratory hot plate until all the wax melted. The solution was waited until

homogeneous then cooled off to room temperature. Again, the typical experiment duration was 10 minutes and three wax deposit measurements was conducted at an interval of one minute for the initial three minutes followed by two measurements taken at an interval of two minutes for the middle four minutes and finally one measurement taken at the end of the experiment time of 10 minutes. After that, the non-crystallized wax-oil was drained out of beaker and weighed. When carrying out measurements of wax deposition, the experiment was stopped and the non-crystallized wax-oil was drained out of beaker and weighed. The crystallized wax inside the beaker was determined by the difference between the weight of the empty beaker and the weight of the beaker with the deposit. After the measurement, the experiment was restarted by recombining the solid deposits with the liquid part and the mixture was reheated to 50°C. The procedure was continued for different types of other solvent apart from diesel such as octane, heptanes and hexane.

3.2 Equipments Used

3.2.1 Leatherhead Food Research Association (LFRA)

The Leatherhead Food Research Association (LFRA) is a type of Universal Testing Machine (UTM). An advantage of LFRA is; same basic machine that could be configured for different kind of tests. The complete force history is plotted giving all the changes that occur, including the rate of change (slopes), maximum force (peaks), fracture events (rapid decreases in force), area under the curve (work) and frequently other parameters of interest. The most common parameters derived from the Texture Profile Analysis (TPA) curve are shown in **Table 5** (Friedman *et al.*, 1963; Bourne, 1968). The peak force during the first compression cycle is defined as hardness. Fracturability (originally called brittleness) is defined as the force at the first significant break in the curve during the first compression cycle. The ratio of the positive force area during the

second compression cycle to that during the first compression cycle (area 2/area 1; **Figure 6**) was originally defined as cohesiveness when using the GF Texturometer. When the Instron is used, cohesiveness is obtained from the areas under the compression portion (downstroke) only and excludes the areas under the decompression portion (upstroke) instead of using the total area under positive force. The negative force area of the first compression cycle (area 3), adhesiveness, is defined as the work necessary to pull the plunger away from the sample. The length to which the sample recovers in height during the time that elapses between the end of the first compression cycle and the start of the second compression cycle is defined as springiness (originally called elasticity). Gumminess is defined as the product of hardness times cohesiveness, and chewiness is defined as the product of hardness times cohesiveness times springiness. For a TPA measurement, make sure that the degree of compression, plunger size, and crosshead speed are the same among tests that are to be compared. The LFRA standard setting that has been used while running the textural analysis of the wax are as follow:

Table 4: LFRA Standard setting

Properties	Value
Probe distance (mm)	5.00
Probe speed (mm/s)	2.00
Cycle Type	Normal
Calibration factor	768003.00
System type	2.00
Probe type	TA10
Load type	Comp

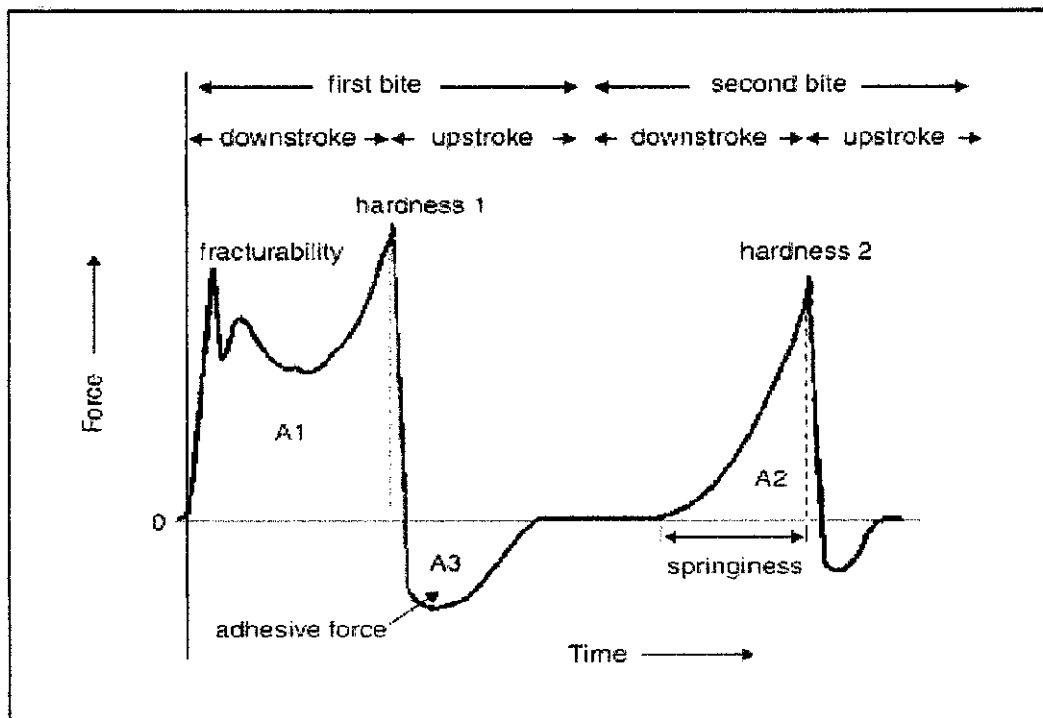


Figure 6: A generalized texture profile analysis curve from the Instron Universal Testing Machine. A1, area 1; A2, area 2; A3, area 3. The dotted lines indicate the times at which hardness is measured (Pons and Fiszman, 1996)

Table 5: Parameters and Units of Instrumental Texture Profile Analysis

Mechanical parameter	Measured variable	S.I. units
Adhesiveness	Work	N × mm (mJ)
Chewiness	Work	N × mm (mJ)
Cohesiveness	Ratio of forces	Dimensionless
Fracturability	Force	N
Gumminess	Force	N
Hardness	Force	N
Springiness	Distance	mm

^aFrom Bourne, 1982.

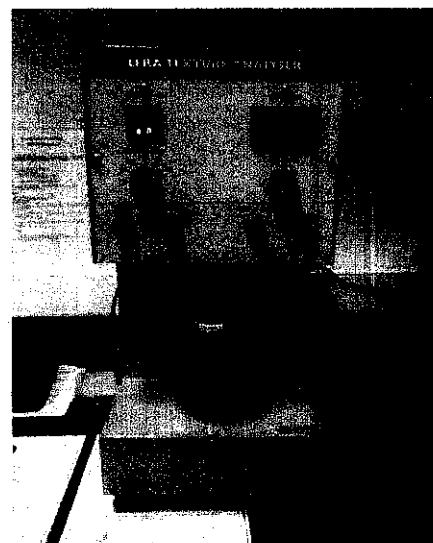


Figure 7: Leatherhead Food Research Association LFRA

3.2.2 Viscometer

A controlled stress viscometer was used for the rheological experiments. Based on the Standard Operating Procedure (SOP) taken from the laboratory, for the start up of the viscometer, after turning on the equipment, select and attach the spindle. Set the spindle number, temperature control and speed control. After that, lower the handle placing the cone onto the plate. Lock the handle into its lowest position and allow around ten minutes for the cone to come to equilibrium temperature with the plate. Later, raise the handle and place the sample to be measured onto the plate below the cone. Lower the handle gently and do not force the spindle onto the plate. The sample must completely cover the face of the spindle and extend beyond the edge of the spindle about 1.0 mm. Allow the spindle, plate and sample to equilibrate to the temperature control setting. Lastly set the run time for rotating the spindle. Press the Run key and execute the viscosity measurement.



Figure 8: Viscometer

3.2.3 Chiller

Used for the experiment effect of temperature differential to achieve the temperature until 2°C



Figure 9: Chiller

3.2.4 Hot water bath

Used for the experiment effect of temperature differential to achieve the temperature up until 80°C

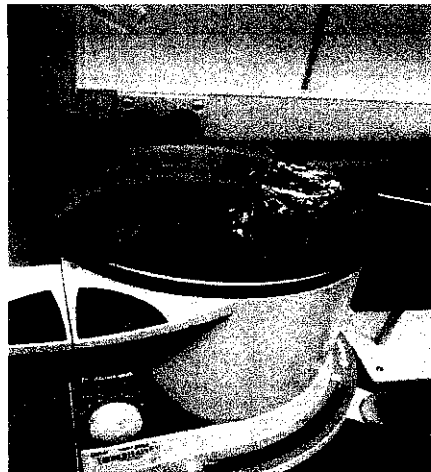


Figure 10: Hot water bath

3.3 Key milestone

3.3.1 Timelines for FYP I

No.	Details/work	1	2	3	4	5	6	7	Mid Semester Break	8	9	10	11	12	13	14	
1	Selection of project topic																
2	Preliminary Research work																
3	Submission of extended proposal defense																
4	Proposal defense																
5	Project work continues																
6	Submission of interim draft report																
7	Submission of interim report																

 Process
 Suggested milestone

3.3.2 Timelines for FYP II

No.	Details/work	1	2	3	4	5	6	7		8	9	10	11	12	13	14	15	
1	Project work continues								Mid Semester Break									
2	Submission of progress report																	
3	Project work continues																	
4	Pre-SEDEX																	
5	Submission of draft report																	
6	Submission of dissertation (soft copy)																	
7	Submission of technical paper																	
8	Oral presentation																	
9	Submission of dissertation (hard bound copy)																	

 Process
 Suggested milestone

CHAPTER 4

RESULTS AND DISCUSSIONS

4.1 Effect of temperature differential

Prior to the study, some initial assumption or hypothesis have been developed to act as a set point to the study. Based on some referred literature, difference in the temperature is higher, the average wax deposition is larger (Guazhong, Z. *et.al.*, 2007). As there are differences in the temperature between the wax-oil solution and the wall temperature, the viscosity behaviors as well as the textural analysis are different accordingly. The data that been gained throughout the studies can be manipulated into tables and graph for the sake of analysis and interpretation.

4.1.1 Fixed T_{max}

For the first experiment, the T_{max} which is the temperature of the wax-oil is fixed to 70°C. Below are the table and graphs of the results obtained. Tables of results for temperature difference 60°C and 55°C are stated in the appendixes.

Table 6: Temperature difference is 65°C. T_{min} is 5°C and T_{max} is 70°C. $M_o=104.16g$

Time(min)	weight	difference	wt%	δr	$\log(-\ln(1-\delta r))$	$\log(t)$
1	116.1	11.94	21.74467	0.217447	-0.61049143	0
2	120.73	16.57	30.17665	0.301767	-0.444661564	0.301
3	129.59	25.43	46.31215	0.463121	-0.206221196	0.477
5	139.77	35.61	64.85158	0.648516	0.019361581	0.699
7	151.74	47.58	86.65088	0.866509	0.303999076	0.845
10	159.07	54.91	100	1	#NUM!	1

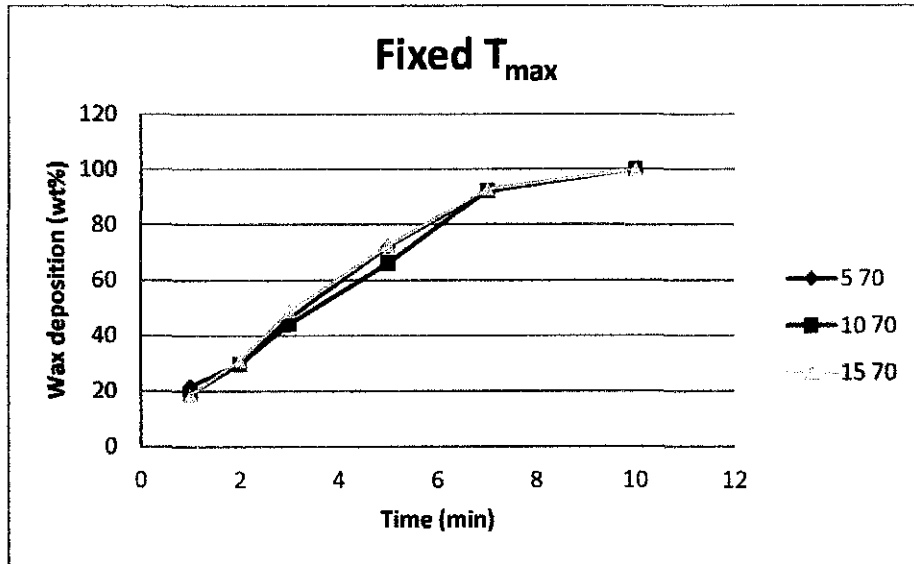


Figure 11: Graph of wax deposits (wt%) vs time for the experiment the effect of temperature differential towards wax crystallization (T_{max} is fixed: 70°C. T_{min} varied: 5, 10, 15°C)

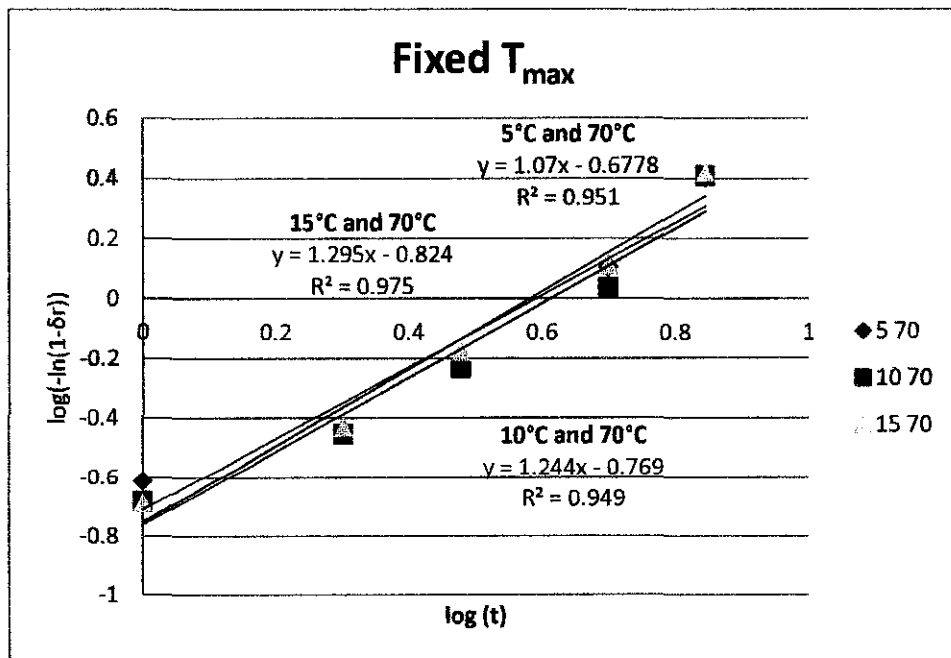


Figure 12: Avrami plot for the experiment the effect of temperature differential towards wax crystallization (T_{max} is fixed: 70°C. T_{min} varied: 5, 10, 15°C)

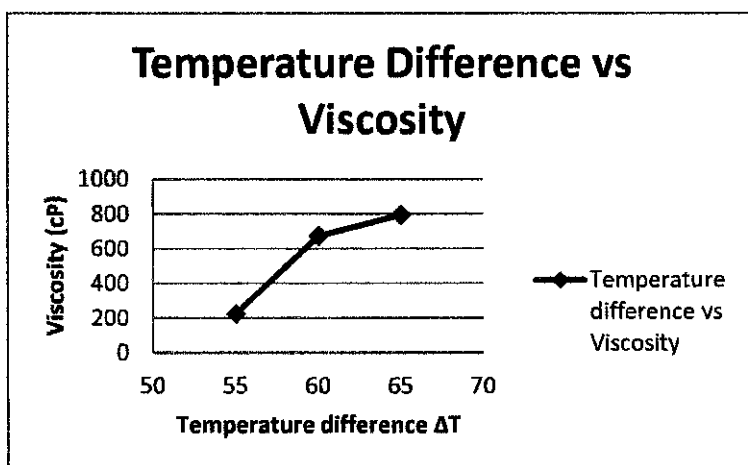


Figure 13: Graph of temperature difference vs viscosity for the experiment effect of temperature differential (Fixed T_{max}). ΔT : 55, 60, 65°C

Table 7: Extracted Avrami parameters for the effect of temperature differential (Fixed T_{max} : 70°C, Varied T_{min} : 5, 10 and 15°C)

Temperature differential ΔT (°C)	n	K (min^{-1})
55	1.295	0.15
60	1.244	0.17
65	1.07	0.21

Based on the results gained in **Figure 11**, we could see that a larger temperature gradient, the more portion of the wax will tend to form precipitation. This shows that our first assumption above is true; higher temperature differential will results in higher wax deposition. From **Figure 13**, we could see that the viscosity is increasing too with the increased of temperature differential. The Avrami parameters are extracted from graph in **Figure 12**. As summarized in **Table 7**, the value of K which is the growth rate of crystallization is increasing as the ΔT is increasing. While the Avrami exponent, n is decreasing with the increased of the value of K but it is approximately equals to 1. Based on the **Table 2** of the Avrami parameters for crystallization as stated in the literature review part above, the value of 1 for Avrami exponent, n suggests that the crystallization mechanism could be rods (constant radius) and the nucleation process could be instantaneous with growth form of 1 dimension

4.1.2 Fixed T_{min}

For the second experiment, the T_{min} which is the wall temperature is fixed to 2°C. Below are the graphs obtained. The tables of result are in appendixes

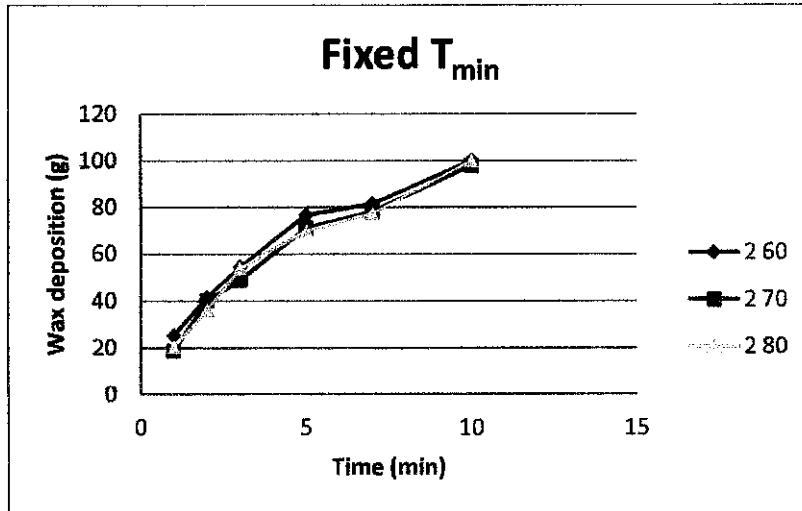


Figure 14: Graph of wax deposits (wt%) vs time for the experiment the effect of temperature differential towards wax crystallization (T_{min} is fixed: 2°C. T_{max} varied: 60, 70, 80°C)

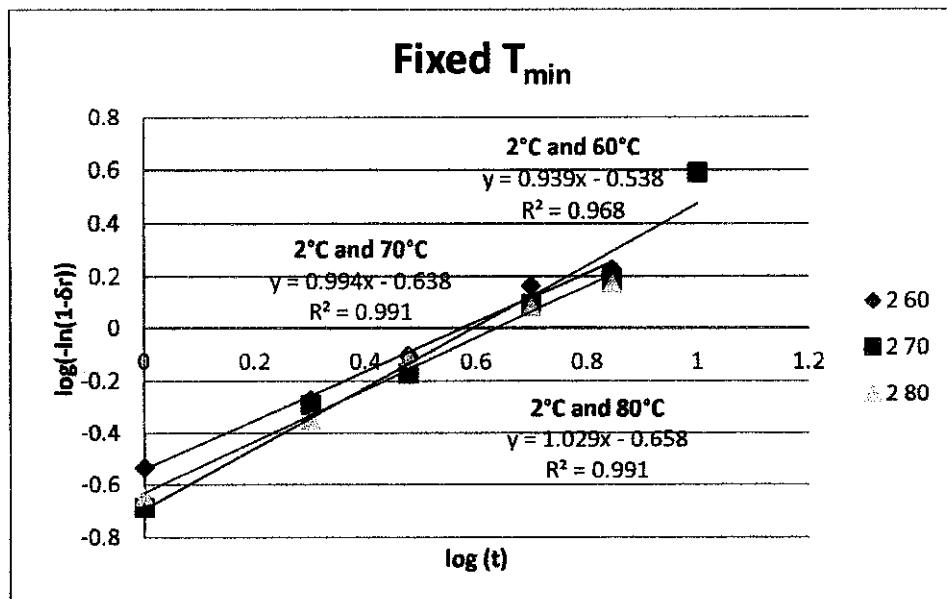


Figure 15: Avrami plot for the experiment the effect of temperature differential towards wax crystallization (T_{min} is fixed: 2°C. T_{min} varied: 60, 70, 80°C)

Table 8: Extracted Avrami parameters for the experiment the effect of temperature differential (Fixed T_{\min} : 2°C. T_{\max} varied: 60, 70 and 80°C)

Temperature differential ΔT (°C)	n	K (min ⁻¹)
58	0.939	0.29
68	0.994	0.23
78	1.029	0.22

For the second experiment, based on graphs in **Figure 14** we could see that the results is opposite with the first experiment where T_{\max} is fixed. Based on the results, as the ΔT increasing, the wax deposition is decreasing. As compared to the first experiment (fixed T_{\max}), the T_{\max} which is the temperature of the wax-oil, wax deposition is increasing with the increased of ΔT and this suggests that as the temperature of the wax-oil is increasing, the amount of the wax deposition could be decreased. This shows that the temperature of the wax-oil and the wall temperature played biggest role for the amount of wax deposition. The Avrami parameters are extracted from graph in **Figure 15**. As summarized in **Table 8**, we could see that the growth rate, K is decreasing as the ΔT is increasing. The value of the Avrami exponent, n is the same as the first experiment which is 1. So the crystallization mechanism could be rods (constant radius) and the nucleation process could be instantaneous with growth form of 1 dimension. However the viscosity measurement for this experiment could not be done because the viscometer in the laboratory only support the temperature range until 5°C.



Figure 16: Wax deposition inside the beaker

4.2 Effect of different wax compositions

Below are the graphs obtained for the experiment the effect of different wax compositions toward the wax depositions. The tables of result are in appendixes.

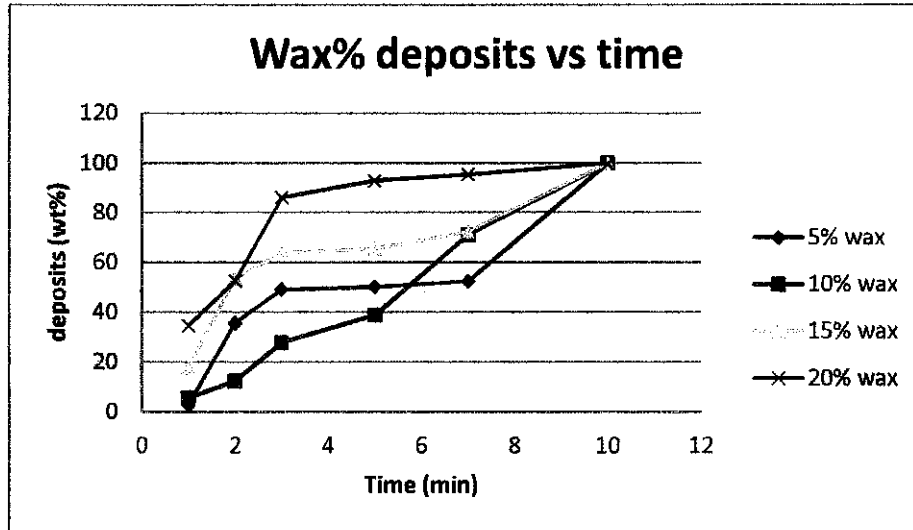


Figure 17: Graph of wax deposits (wt%) vs time (min) for the experiment the effect of different wax composition towards wax crystallization (wax compositions: 5, 10, 15 and 20%)

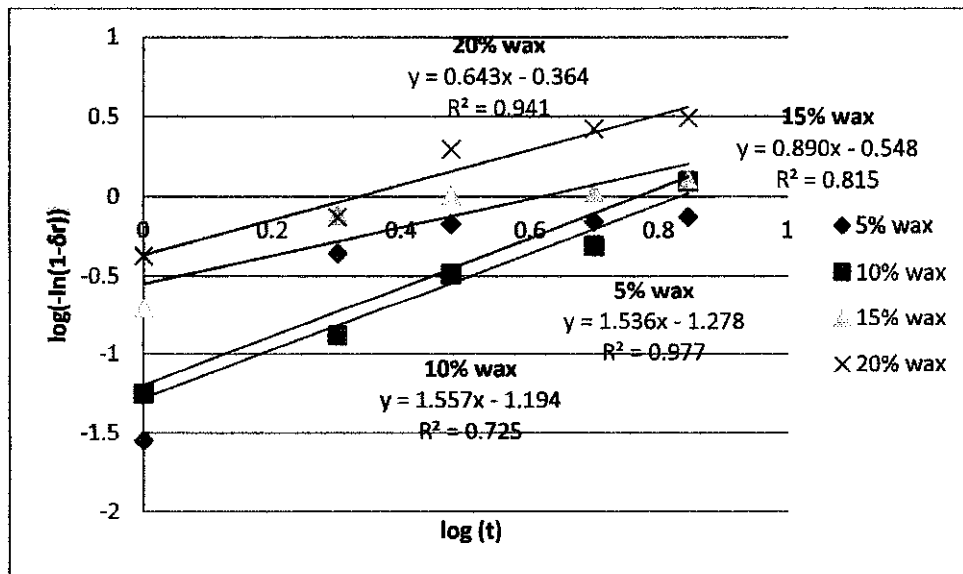


Figure 18: Avrami Plot for the experiment effect of different wax composition towards wax crystallization (wax compositions: 5, 10, 15 and 20%. Model oil: Diesel)

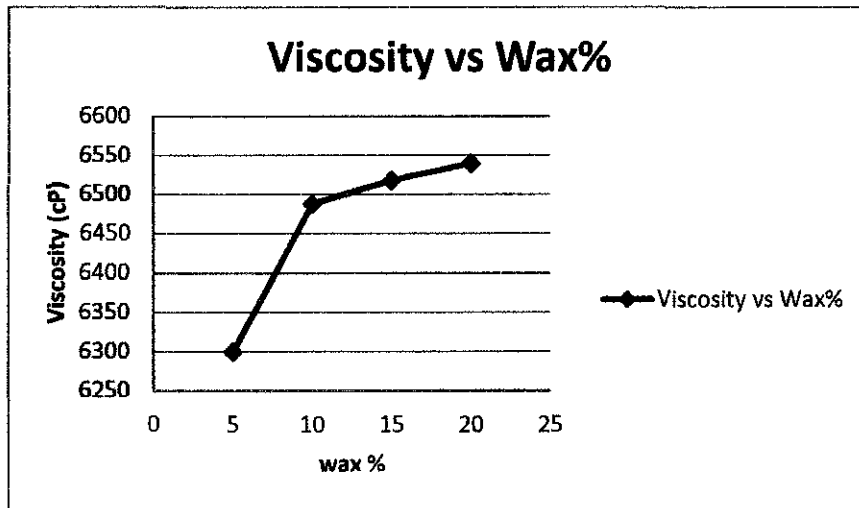


Figure 19: Graphs of viscosity vs wax composition (wax compositions: 5, 10, 15 and 20%. Model oil: Diesel)

Table 9: Extracted Avrami parameters for the experiment the effect of wax composition. (Wax compositions: 2, 10, 15 and 20%. Model-oil: Diesel)

Wax Content (wt%)	n	K (min^{-1})
5	2.314	0.038
10	1.536	0.053
15	0.890	0.283
20	0.643	0.433

From the graphs obtained in **Figure 17**, we could see clearly that as the wax composition increases, the more wax deposits produced at any given time, the faster the deposition rates and the faster it reaches the 100% wax deposition. These results are well expected because as the paraffin wax in the solution is increases, there are more wax molecules available to produce the wax crystals. The higher wax composition, the larger rate of deposition will takes place. This analysis show whenever crude oil comes with larger composition of wax there will be higher rate of deposition of wax and the maintenancewill be harder.As for the viscosity, based on the graph in **Figure 19**, it is increasing as the wax composition increasing. This is also well expected because as there is larger amount of wax crystallize will resulting in the increment of the viscosity as the interaction between the wax-oil molecules act as a resistance to the flow. The Avrami parameters are extracted from graph in **Figure 18**. As summarized in **Table 9**,

we could see that the growth rate, K is generally increasing with the wax content in solution or supersaturation level. Even based on observations, the amount of crystals crystallized for the 5% wax composition is too little and the rate of crystallization is lower compared to the solution that contained 20% wax composition. This is because as the higher wax concentration or supersaturation, the more wax crystals, the higher crystallization rate. The Avrami exponent, n decreases with the increase of the wax concentration. This suggests that there are different growth forms of crystals for different wax compositions. For example, for the 5% wax composition, the value of n is 2 which shows that the crystallization mechanism could be either disc (constant thickness) and instantaneous and the growth form could be two dimensions or rods (constant radius) and sporadic and the growth form could be one dimension (Hay, 1971)

4.3 Effect of different types of solvents

Below are the graphs obtained for the experiment the effect of different type of solvents toward the wax depositions. The tables of results are in appendixes.

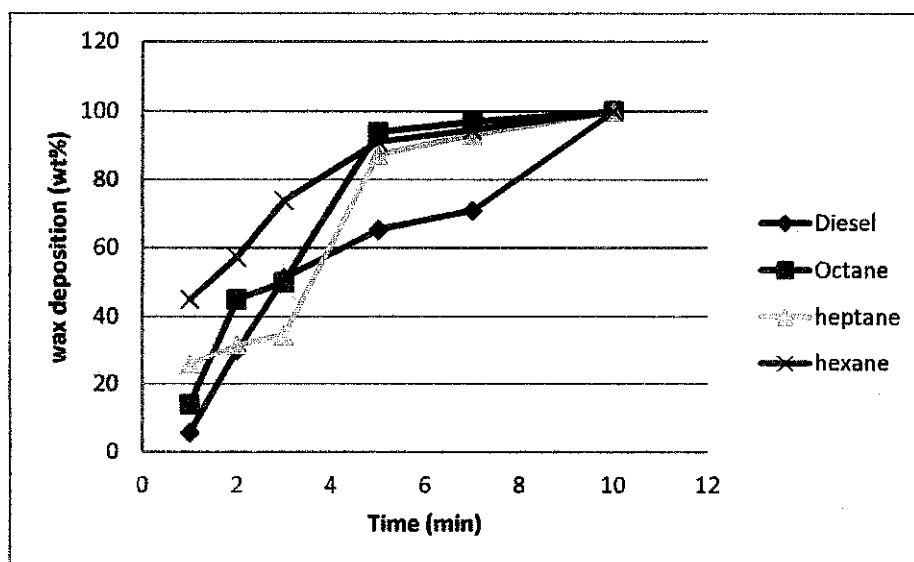


Figure 20: Graph of wax deposits (wt%) vs time (min) for the experiment the effect of different types of solvents towards wax crystallization (Solvents: Diesel, Octane, Heptane and Hexane. Wax composition: 17%)

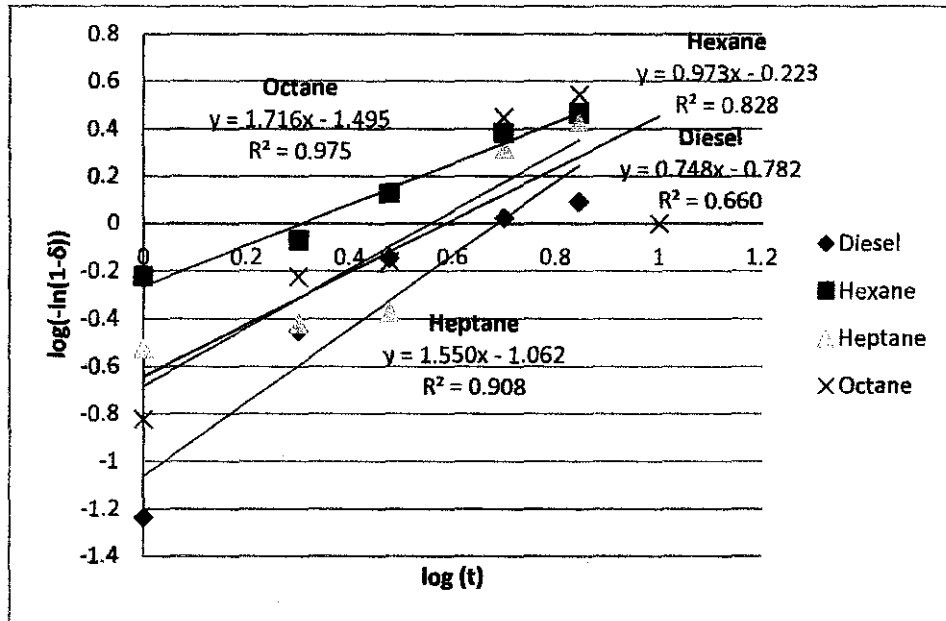


Figure 21: Avrami Plot for the experiment the effect of different types of solvents towards wax crystallization (Solvents: Diesel, Octane, Heptane and Hexane. Wax composition: 17%)

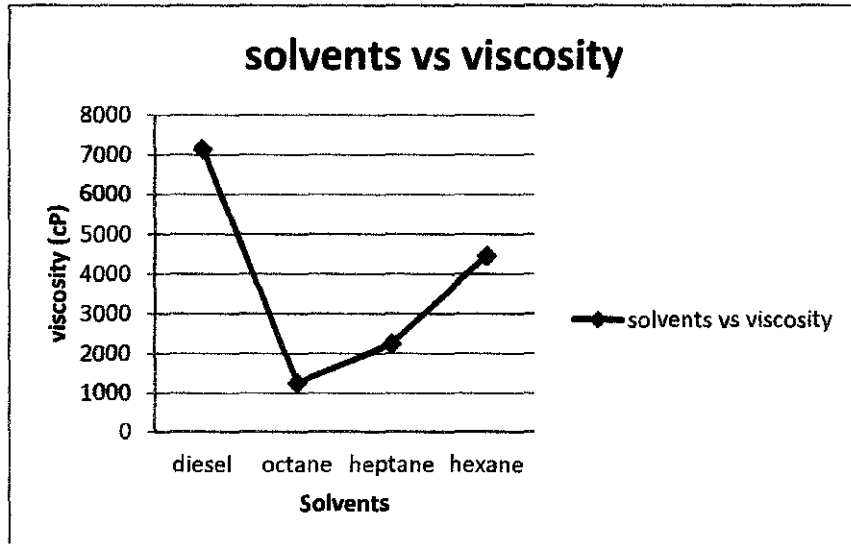


Figure 22: Graphs of solvent vs viscosity for the experiment the effect of different types of solvents towards the wax crystallization. (Solvents: Diesel, Octane, Heptane and Hexane. Wax composition: 17%)

Table 10: Extracted Avrami parameters for the experiment the effect of different types of solvents towards the wax crystallization. (Solvents: Diesel, Octane, Heptane and Hexane. Wax composition: 17%)

Solvents	n	K (min⁻¹)
Diesel	0.748	0.782
Octane	1.716	0.032
Heptane	1.550	0.21
Hexane	0.973	0.598

Based on the **Figure 20**, we could see that, the wax crystallization is higher for diesel followed by hexane, heptane and octane. Even based on observation, the sign of wax crystallize could be seen even faster in diesel than any other solvents. Theoretically, the carbon chain for diesel ($C_{12}H_{23}$) is the highest followed by octane (C_8H_{18}), heptane (C_7H_{16}) and hexane (C_6H_{14}). First assumption is the wax deposition is higher as the carbon chain is increasing but according to the results, as the carbon chain is increasing, the wax deposition is decreasing except for solvent diesel. The Avrami parameters are extracted from graph in **Figure 21**. As summarized in **Table 10**, the growth rate, K is decreasing with the increase of carbon chain except for solvent diesel where the growth rate is the highest. As the carbon chain increasing from hexane to octane, the value of the Avrami exponent, n is increasing. As for viscosity in **Figure 22**, the viscosity is highest in Diesel and started to decrease as the carbon chain increasing from hexane to octane. The trend of wax crystallization is different in diesel than other solvents could be due to other components in the diesel itself such as additives. However, it is not fully understood of why this growth rate and crystallization mechanism behave differently with the changes of carbon chain in the solvent.

4.4 LFRA Texture Analysis

Samples from the experiments have been tested with LFRA Texture Analyzer in order to investigate the effects of all those parameters towards the hardness, break load and adhesive force of the wax deposits.

4.4.1 Effect of different wax compositions

Below is the result obtained from the LFRA Texture Analyzer. Results from LFRA Texture Analyzer for other wax compositions are stated in the appendixes.

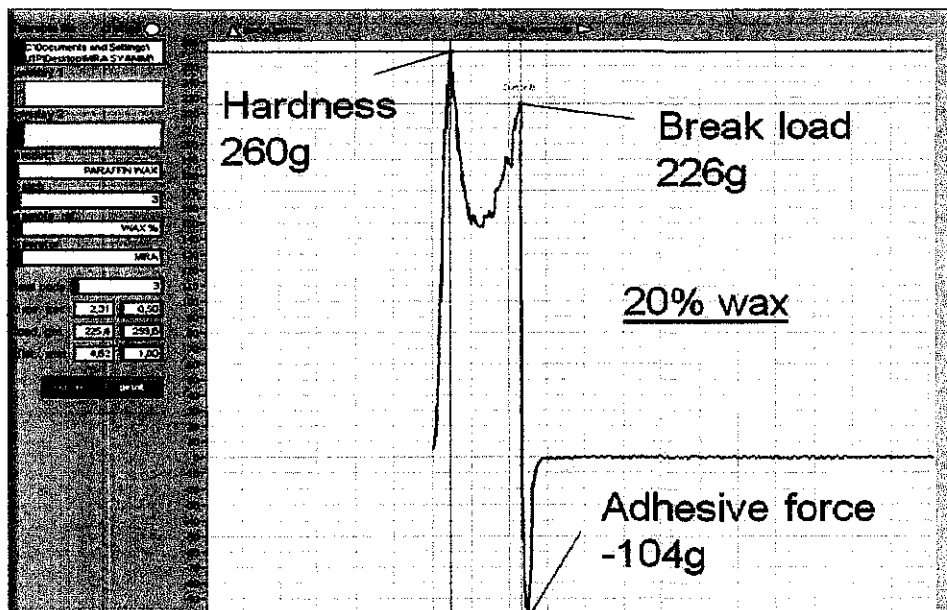


Figure 23: Graph of texture analysis from LFRA Texture Analyzer for the experiment effect of different wax composition. Wax compositions: 20%. Model-oil used: Diesel.

Table 11: Texture analysis for effect of different wax compositions

Wax compositions	Hardness	Adhesive force	Break load
5	13	-8	13
10	98	-39	94
15	181	-63	181
20	260	-104	226

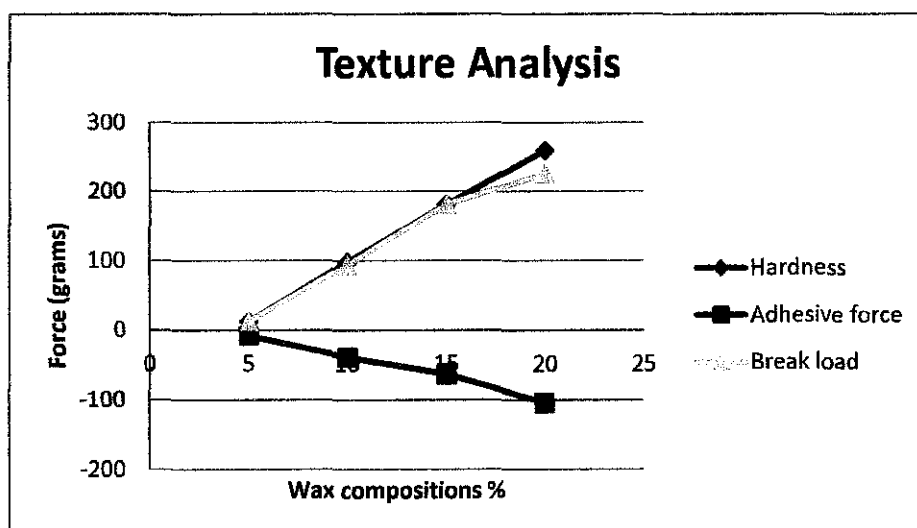


Figure 24: Graphs of texture analysis for the experiment effect of different wax compositions. (Wax composition: 5, 10, 15 and 20%. Model-oil used: Diesel)

Figure 23 shows the trend of graph obtained from LFRA and from the graph the data of hardness, break load and adhesive force are obtained and plotted as in **Figure 24**. The data obtained has been summarized in **Table 11**. From the graph in **Figure 24**, as the wax composition is increasing, the hardness is increasing too. It makes sense as there is more wax molecule available and more crystallization that will occur making more bonding thus will increase the hardness. Break load is the tensile or compressive load required to fracture or to cause the sample to fail. As for the break load, it is linearly increasing too with the increase of hardness. The reason is also the same where there is more wax molecule available and more crystallization that will occur making more bonding thus will increase the break load. Adhesive forces are the attractive forces between different molecules. They are caused by forces acting by two substances. So as the wax composition in the solvent is increasing, the adhesive force between the wax and the solvent will decrease as there are more bonding between the wax molecules itself.

4.4.2 Effect of different type of solvents

Below is the results obtained from the LFRA Texture Analyzer. Results from LFRA Texture Analyzer for other types of solvents are stated in the appendixes.

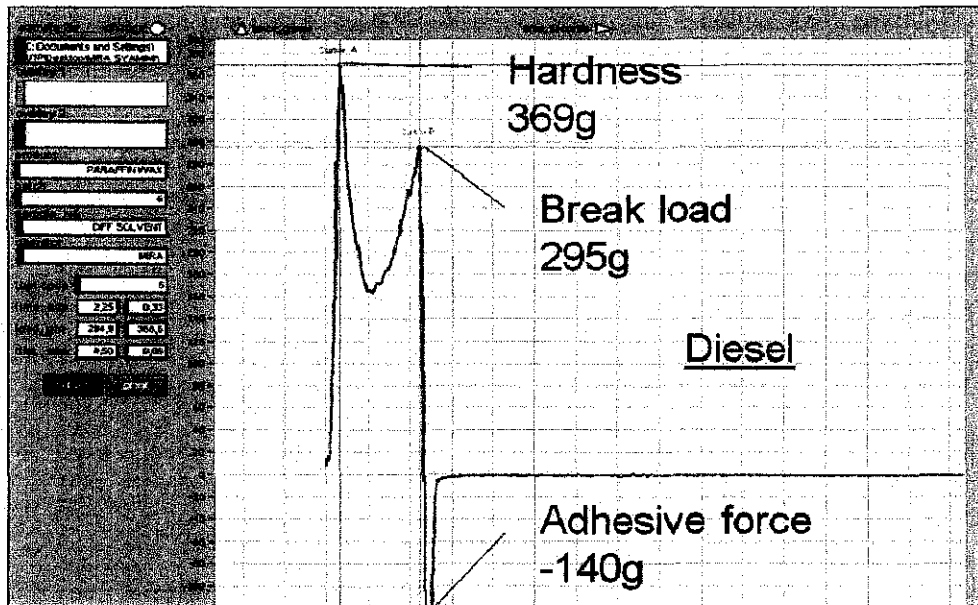


Figure 25: Graph of texture analysis from LFRA Texture Analyzer for the experiment effect of different type of solvents. Solvent used: Diesel. Wax composition: 17%

Table 12: Texture analysis for different type of solvents

Solvents	Hardness	Adhesive force	Break load
Diesel	369	-140	295
octane	30	-16	30
heptane	46	-25	46
hexane	154	-102	196

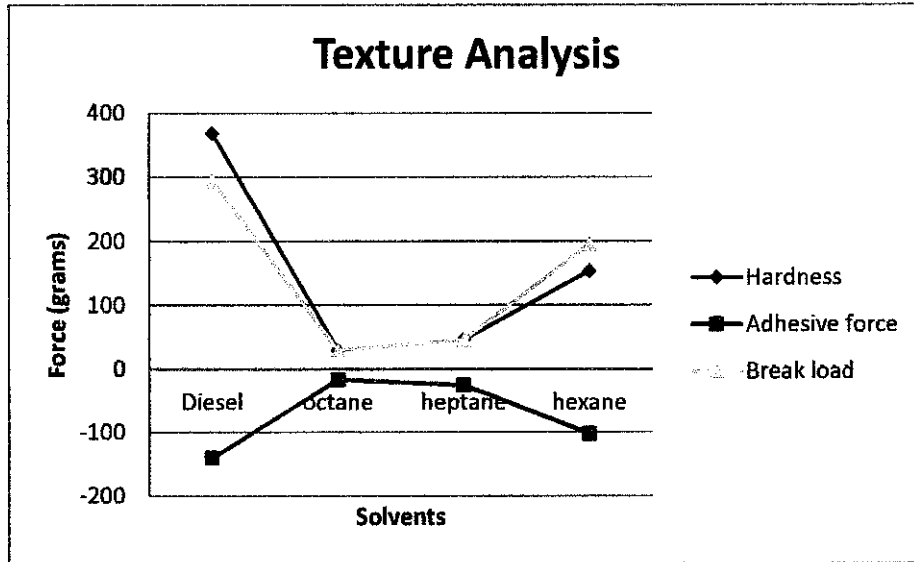


Figure 26: Graph of texture analysis for the experiment effect of different type of solvents. (Solvents used: Diesel, Octane, Heptane and Hexane). Wax composition: 17%

Figure 25 shows the trend of graph obtained from LFRA and from the graph the data of hardness, break load and adhesive force are obtained and plotted as in **Figure 26**. The data obtained has been summarized in **Table 12**. From the graph in **Figure 26**, the hardness for the sample with the solvent diesel is highest among all. For the sample with the solvent octane, heptanes and hexane, the hardness is increase as the carbon chain of the solvents is decreasing. The result for break load is linearly the same as the results for hardness. While adhesive force is decreasing starting from octane, heptanes and hexane which shows that the adhesive force is decreasing with the decrease of the number of carbon chain of the solvents

CHAPTER 5

CONCLUSION AND RECOMMENDATION

5.1 Conclusions

All the objectives for this project have been achieved where firstly is to study the effect of the temperature differential, effect of different wax compositions and to study the effect of different type of solvents towards the wax crystallization. And after that, the samples have been tested with the LFRA Texture Analyzer as well as viscometer and the results of the texture analysis and viscosity of each sample have also been achieved. It shows that, due to all the effects studied, there are changes in hardness, adhesive force and break load of each sample. The major conclusions of this work are summarized as follows:

1. For the effect of temperature differential, for the experiment with fixed T_{\max} , the results are as expected where higher ΔT will result in more wax deposition and increasing trend for the viscosity. But the results for the experiment with fixed T_{\min} shows an opposite trend where higher ΔT with the increase of T_{\max} will result in lower wax deposition and the viscosity is decreasing.
2. As for the effect of different wax composition, the results obtained are as expected where higher wax composition will result in higher wax deposition and increased in viscosity. Based on the results from LFRA Texture Analyzer, the hardness and the break load of the wax crystallization are increasing with the increased of the wax composition while the adhesive force is decreasing.
3. Lastly, for the effect of different type of solvents, the wax deposition is highest in the solvent diesel but it is increasing with the decreasing of the number of carbon chain of the solvents starting from octane, heptane and hexane. For texture analysis, based on the results from LFRA Texture Analyzer, the hardness and break load of the wax crystallization is highest in the solvent diesel and started to decrease as the carbon number is increasing from hexane, heptane to octane. For the adhesive force, it is lowest in the solvent diesel but

started to increase with the increased of the carbon chain in the solvent starting from hexane, heptane to octane.

4. With the results obtained, the rate and mechanism of crystallization has been studied with accordance to the Avrami theory. Based on the results, as the wax deposition increased the value of growth rate, K will increase too while the value of Avrami exponent, n will decrease. It shows that there are different mechanisms of crystallization due to the effect of certain parameters. However the value are mostly fractional values and it suggests that it is due to secondary crystallization for example lower n values (<1) are caused by linear growth (Pal S. *et al.*, 2005)

5.2 Recommendation

This study could provide a solution in order to control the formation of the precipitation. The identification of the temperature range that makes the formation of the precipitation to occur will be very useful for the industries. Knowledge of the magnitude of wax deposition can lead to reduction of insulation requirement for production and transportation systems. Conversely, problems with wax can be addressed at the early stage of a project so that sufficient thermal insulation could be planned for instead of expensive chemical injection and loss in the production capacity. The minimum pigging frequency can be determined if the amount of wax deposition can be estimated. In addition, the problems related to wax deposition can be solved in more effective manner if the effects of the wax deposition are further studied and understand.

For further enhancement, simulation model could be developed for simulating wax deposition in pipe. Many researches have studied the thermodynamic of wax deposition in hopes of creating a model that accurately describes the process. For example in earlier work, Lira-Galeana *et al.* (1996) developed thermodynamic framework for calculating wax precipitation in petroleum mixtures as several distinct solid phases. Solaimany *et al.* (1996) later developed a multi-solid phase thermodynamic model for predicting wax precipitation in petroleum mixtures by using

the Peng-Robinson equation of state to evaluate the phase behaviour of both liquid and vapour phases. Besides, Ramirez-Jaramillo *et al.* (2004) developed a multi-component liquid-wax hydrodynamic model for simulating wax deposition in pipelines which treated molecular diffusion as the dominant mechanism. In future, for this work we could work out on the simulation model that consisting of a model pipe along with a mixture of hydrocarbons flow.

The knowledge of Transport Phenomena before this could also be applied in this work by applying certain boundary conditions at the end and along the exterior surface of the pipe. The wax deposition rate could be considered to depend on oil composition, oil temperature, external temperature around the pipe, flow condition, pipelines size and pressure.

REFERENCES

- Ararimeh, A., Dhurjati Prasad Chakrabarti, Angelus Pilgrim, Sastry, M.K.S. (2010). Wax Formation on oil pipeline, The University of West Indies, 246-278.
- Avrami, M. (1940). Kinetics of Phase Change II. Transformation-Time Relations for Random Distribution of Nuclei. *Journal of Chemical Physics*. 212-224.
- Azevedo, L.F.A, Teixeira, A.M. (2003). A critical review of the modeling of wax deposition mechanism, *Petro. Sci. Technol*, 393-408.
- Bott, T.R. and Gudmunson, J.S. (1978). Operation of paraffin wax flowing system., Institute of petroleum, IP77-007, London, 198-210.
- Burger, Perkin and Wrinkles, J (1965). Studies of Wax Deposition in the Trans Alaska pipeline. *Journal of Petroleum Technology*, 1075-1086.
- Guzhong, Z., Gang, L. (2007). Study on the Wax deposition of Waxy Crude in pipelines and its application, China University of Petroleum, 78-91.
- Ismail. L., Westacott. R.E., Ni. X. (2008). On the Effect of wax content on paraffin deposition in a batch oscillatory baffled tube apparatus, 205-213.
- Hay, J.N. (1971). Application of the modified Avrami equations to polymer crystallization kinetics, *Br. Polym. J.* 3 (2) 74-82.
- Lira-Galeana, C., Firoozabadi, A., Prausnitz, J.M. (1996). Thermodynamic of wax precipitation in petroleum mixtures, *AIChE J.* 42, 239-248.

- Paso, K., Senra, M., Yi, Y., Sastry, A.M., Fogler, H.S. (2005). Paraffin Polydispersity Facilitates Mechanical Gelation, University of Michigan, 478-491.
- Pederson, K.S., Ronningsen, H.P. (2003). Influence of Wax Inhibitor on wax Appearance Temperature, Pour point and viscosity of waxy crude oils. Energy Fuels, 321-328.
- Ramirez-Jaramillo, E., Lira-Galeana, C., Manero, O. (2001). Numerical simulation of wax deposition in oil pipeline systems, Petrol. Sci. Technol. 19, 143-156.
- Richter, D., Radulescu, A., Schwan, D. (1996). Wax Control by Self Assembling Polymer, Germany, 97-103.
- Sharples, A. (1966). Overall kinetics of crystallisation Pages 44-59 in Introduction to Polymer Crystallisation. A. Sharples, ed. Edward Arnold Ltd. London.
- Singh, P., Venkatesan, R. Fogler, H.S and Nagarajan, N.R. (2001). Morphological Evolution of Thick Wax deposit during Aging, 6-18.
- Solaimany, A.R., Dabir, B., Islam, M.R. (2005). Experimental and mathematical modelling of wax deposition and propagation in pipes transporting crude oil. Energy Source 27, 185-207.

APPENDIXES

6.1 Effect of temperature differential

Below are tables of results for the experiment the effect of temperature differential towards wax crystallization. (Fixed T_{\min} and Fixed T_{\max})

Table 1: Temperature difference is 10°C and 70°C. Mo= 104.16g

Time(min)	weight	difference	wt%	δr	$\log(-\ln(1-\delta r))$	$\log(t)$
1	114.02	9.86	18.89613	0.188961	-0.678941424	0
2	119.67	15.51	29.72403	0.29724	-0.452544923	0.301
3	127.28	23.12	44.30816	0.443082	-0.232594303	0.477
5	138.71	34.55	66.21311	0.662131	0.035468676	0.699
7	152.34	48.18	92.33423	0.923342	0.409663493	0.845
10	156.34	52.18	100	1	#NUM!	1

Table 2: Temperature difference is 15°C and 70°C. Mo= 104.16g

Time(min)	weight	difference	wt%	δr	$\log(-\ln(1-\delta r))$	$\log(t)$
1	113.39	9.23	18.66909	0.186691	-0.684777006	0
2	119.52	15.36	31.06796	0.31068	-0.429399729	0.301
3	128.24	24.08	48.7055	0.487055	-0.175492335	0.477
5	140.07	35.91	72.6335	0.726335	0.112554857	0.699
7	150.09	45.93	92.90049	0.929005	0.422449283	0.845
10	153.6	49.44	100	1	#NUM!	1

Table 3: Temperature difference is 2°C and 60°C. Mo=104.16g

Time(min)	weight	difference	wt%	δr	$\log(-\ln(1-\delta r))$	$\log(t)$
1	118.34	14.15	25.44506	0.254451	-0.532193756	0
2	127.29	23.1	41.53929	0.415393	-0.270175109	0.301
3	134.57	30.38	54.63046	0.546305	-0.102191929	0.477
5	146.92	42.73	76.8387	0.768387	0.165151497	0.699
7	149.56	45.37	81.58605	0.81586	0.228416124	0.845
10	159.95	55.76	100.2697	1.002697	#NUM!	1

Table 4: Temperature difference is 2°C and 70°C. Mo= 104.16g

Time(min)	weight	difference	wt%	δr	$\log(-\ln(1-\delta r))$	$\log(t)$
1	114.57	10.38	18.65229	0.186523	-0.685211375	0
2	126.54	22.35	40.16173	0.401617	-0.289438679	0.301
3	131.49	27.3	49.0566	0.490566	-0.171046991	0.477
5	143.8	39.61	71.177	0.71177	0.09481915	0.699
7	147.76	43.57	78.2929	0.782929	0.18399	0.845
10	158.72	54.53	97.98742	0.979874	0.591704819	1

Table 5: Temperature difference is 2°C and 80°C. Mo= 104.16g

Time(min)	weight	difference	wt%	δr	$\log(-\ln(1-\delta r))$	$\log(t)$
1	115.06	10.87	20.34057	0.203406	-0.64319092	0
2	123.54	19.35	36.20883	0.362088	-0.34721674	0.301
3	132.97	28.78	53.85479	0.538548	-0.11160873	0.477
5	141.67	37.48	70.13473	0.701347	0.082237289	0.699
7	145.65	41.46	77.58234	0.775823	0.174734414	0.845
10	157.63	53.44	100	1	#NUM!	1

6.2 Effect of different wax compositions

Below are the tables of results for the experiment the effect of different wax compositions towards wax crystallization. Wax compositions: 5, 10, 15 and 20%

Table 6: Wax composition of 5% wax (2.5 gram). Mo=103.45 gram

Time(min)	weight	difference	wt%	δr	$\log(-\ln(1-\delta r))$	$\log(t)$
1	103.5	0.05	2.793296	0.027933	-1.54774566	0
2	104.09	0.64	35.75419	0.357542	-0.35413219	0.30103
3	104.33	0.88	49.16201	0.49162	-0.16971532	0.477121
5	104.35	0.9	50.27933	0.502793	-0.15567853	0.69897
7	104.39	0.94	52.51397	0.52514	-0.1279985	0.845098
10	105.24	1.79	100	1	1.519144145	1

Table 7: Wax composition of 10% wax (5 gram). Mo=107.23 gram

Time(min)	weight	difference	wt%	δr	$\log(-\ln(1-\delta r))$	$\log(t)$
1	108.89	1.66	5.522289	0.055223	-1.24560396	0
2	110.96	3.73	12.40852	0.124085	-0.87782867	0.30103
3	115.6	8.37	27.84431	0.278443	-0.48632429	0.477121
5	118.92	11.69	38.88889	0.388889	-0.3076145	0.69897
7	128.62	21.39	71.15768	0.711577	0.094585223	0.845098
10	137.29	30.06	100	1	#NUM!	1

Table 8: Wax composition of 15% wax (7.5 gram). Mo=104.17 gram

Time(min)	weight	difference	wt%	δr	$\log(-\ln(1-\delta r))$	$\log(t)$
1	110.61	6.44	17.94372	0.179437	-0.70385102	0
2	123.4	19.23	53.58038	0.535804	-0.114951	0.30103
3	127.07	22.9	63.80607	0.638061	0.007012898	0.477121
5	127.71	23.54	65.5893	0.655893	0.028084083	0.69897
7	130.15	25.98	72.38785	0.723879	0.109549646	0.845098
10	140.06	35.89	100	1	#NUM!	1

Table 9: Wax composition of 20% wax (10 gram). Mo=99.27 gram

Time(min)	weight	difference	wt%	δr	$\log(-\ln(1-\delta r))$	$\log(t)$
1	117.01	17.74	34.70266	0.347027	-0.3703673	0
2	126.15	26.88	52.58216	0.525822	-0.12716126	0.30103
3	143.35	44.08	86.22848	0.862285	0.297228013	0.477121
5	146.83	47.56	93.03599	0.93036	0.425601913	0.69897
7	148.12	48.85	95.55947	0.955595	0.49337383	0.845098
10	150.39	51.12	100	1	#NUM!	1

6.2 Effect of different type of solvents

Below are the tables of results for the experiment the effect of different type of solvents towards wax crystallization. Wax composition used is fixed: 17%

Table 10: Solvent used= Hexane. Mo=107.98g

Time(min)	weight	Difference	wt%	δr	$\log(-\ln(1-\delta r))$	$\log(t)$
1	113.35	5.37	45.08816121	0.450881612	-0.222253398	0
2	114.81	6.83	57.34676742	0.573467674	-0.069526192	0.30103
3	118.79	10.81	90.76406381	0.907640638	0.376954192	0.477121

5	116.84	8.86	74.39126784	0.743912678	0.134252606	0.69897
7	119.25	11.27	94.6263644	0.946263644	0.465927681	0.845098
10	119.89	11.91	100	1	#NUM!	1

Table 11: Solvent used= Octane. Mo= 101.53g

Time(min)	weight	Difference	wt%	δr	$\log(-\ln(1-\delta r))$	$\log(t)$
1	101.67	0.14	2.626641651	0.026266417	-1.574832068	0
2	101.98	0.45	8.442776735	0.084427767	-1.054501782	0.30103
3	102.03	0.5	9.380863039	0.09380863	-1.006542736	0.477121
5	102.47	0.94	17.63602251	0.176360225	-0.712148998	0.69897
7	102.5	0.97	18.1988743	0.181988743	-0.697065071	0.845098
10	102.53	1	18.76172608	0.187617261	-0.682388533	1

Table 12: Solvent used= Diesel. Mo=97.79g

Time(min)	weight	Difference	wt%	δr	$\log(-\ln(1-\delta r))$	$\log(t)$
1	100.17	2.38	5.653206651	0.056532067	-1.235129988	0
2	110.4	12.61	29.95249406	0.299524941	-0.44855425	0.30103
3	119.33	21.54	51.16389549	0.511638955	-0.144662414	0.477121
5	125.27	27.48	65.27315914	0.652731591	0.024344966	0.69897
7	127.68	29.89	70.9976247	0.709976247	0.09264783	0.845098
10	139.89	42.1	100	1	#NUM!	1

Table 13: Solvent used= Heptane. Mo=99.27g

Time(min)	weight	Difference	wt%	δr	$\log(-\ln(1-\delta r))$	$\log(t)$
1	99.54	0.27	25.96153846	0.259615385	-0.522032006	0
2	99.6	0.33	31.73076923	0.317307692	-0.418265299	0.30103
3	99.63	0.36	34.61538462	0.346153846	-0.371730447	0.477121
5	100.18	0.91	87.5	0.875	0.317946716	0.69897
7	100.24	0.97	93.26923077	0.932692308	0.431119324	0.845098
10	100.31	1.04	100	1	#NUM!	1

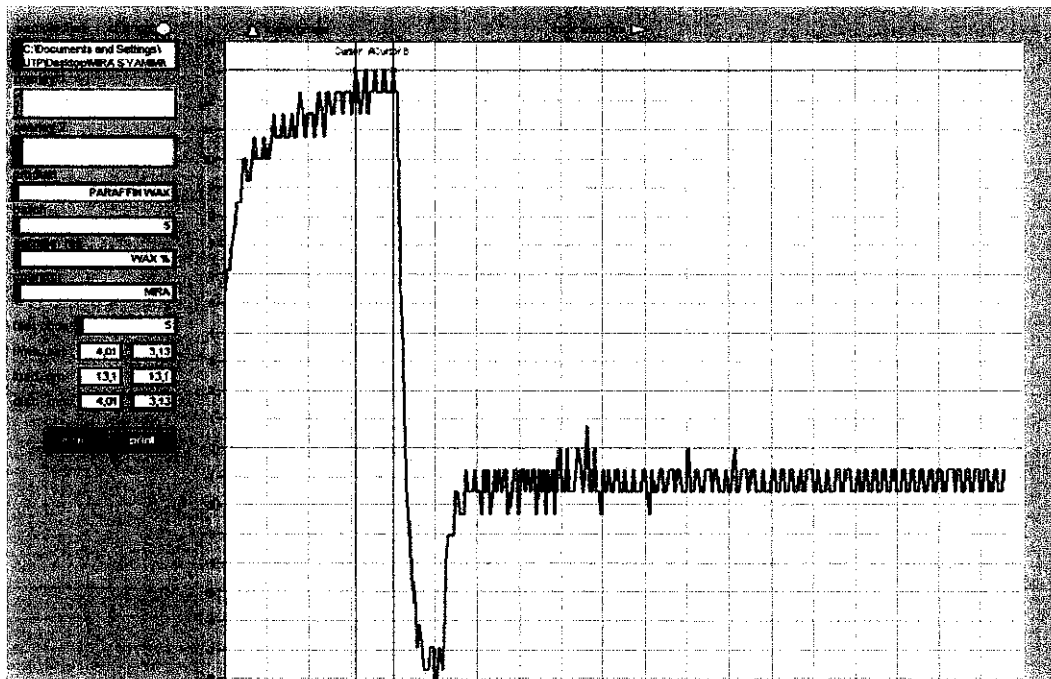


Figure 1: Graph of texture analysis from LFRA Texture Analyzer for the experiment effect of different wax composition. Wax composition: 5% wax Model-oil used: Diesel.

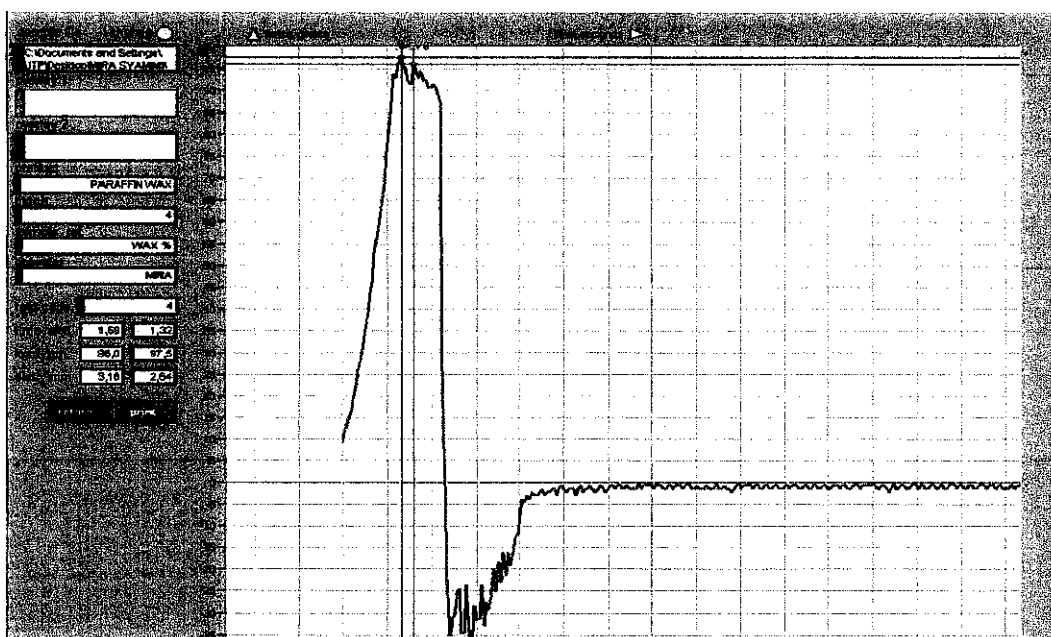


Figure 2: Graph of texture analysis from LFRA Texture Analyzer for for the experiment effect of different wax composition. Wax composition: 10% wax Model-oil used: Diesel.

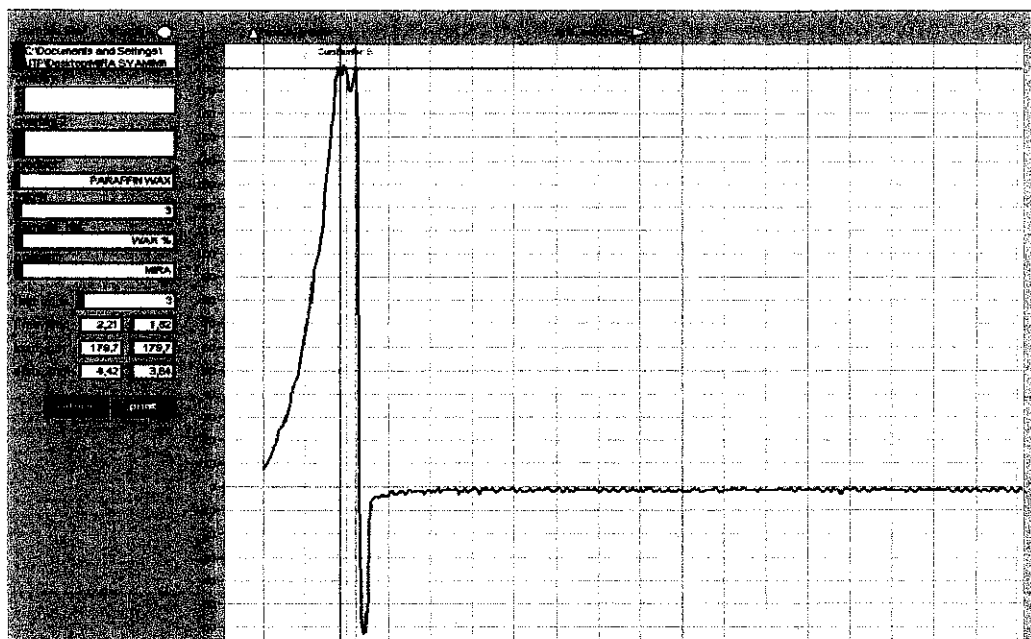


Figure 3: Graph of texture analysis from LFRA Texture Analyzer for for the experiment effect of different wax composition. Wax composition: 15% wax Model-oil used: Diesel.

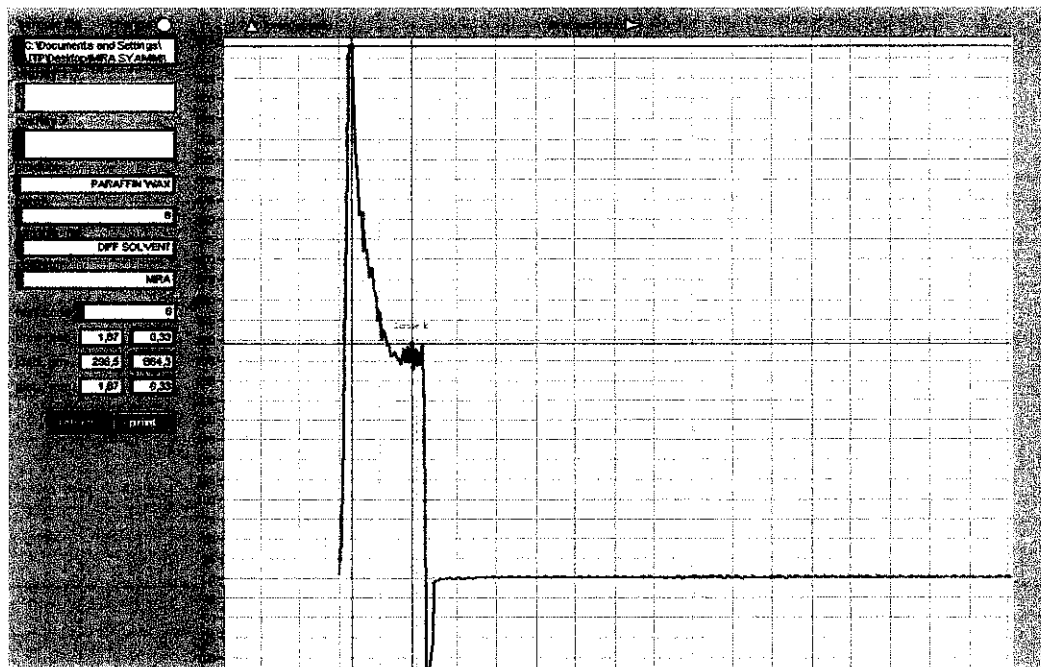


Figure 4: Graph of texture analysis from LFRA Texture Analyzer for the experiment effect of different types of solvents. Solvent used: Hexane. Wax composition: 17%

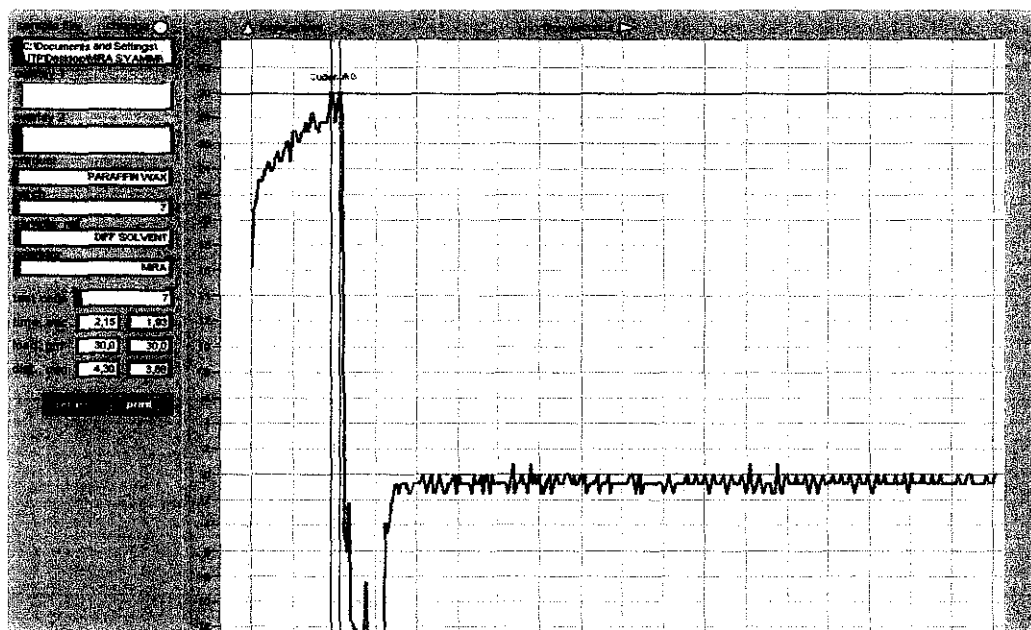


Figure 5: Graph of texture analysis from LFRA Texture Analyzer for the experiment effect of different types of solvents. Solvent used: Octane. Wax composition: 17%

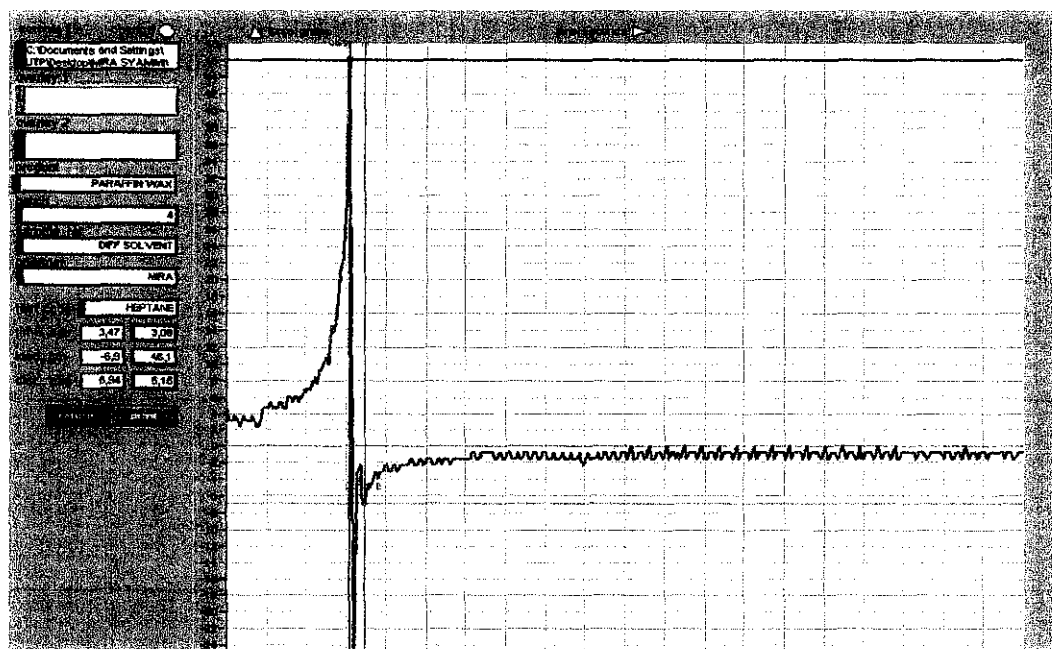


Figure 6: Graph of texture analysis from LFRA Texture Analyzer for the experiment effect of different types of solvents. Solvent used: Heptane. Wax composition: 17%